Evaluating congestion pricing schemes using agent-based passenger and freight microsimulation

Jing, Peiyu; Seshadri, Ravi; Sakai, Takanori; Shamshiripour, Ali; Alho, Andre Romano; Lentzakis, Antonios; Ben-Akiva, Moshe E.

Published in:
Transportation Research Part A: Policy and Practice

Link to article, DOI:
10.1016/j.tra.2024.104118

Publication date:
2024

Document Version
Publisher's PDF, also known as Version of record

Transportation Research Part A 186 (2024) 104118

Contents lists available at ScienceDirect

Transportation Research Part A

journal homepage: www.elsevier.com/locate/tra

Evaluating congestion pricing schemes using agent-based passenger and freight microsimulation

Peiyu Jing [a], Ravi Seshadri [b,*], Takanori Sakai [c], Ali Shamshiripour [a], Andre Romano Alho [a], Antonios Lentzakis [a], Moshe E. Ben-Akiva [a]

[a] Civil and Environmental Engineering Department, Massachusetts Institute of Technology, Cambridge, MA, United States of America
[b] Department of Technology, Management and Economics, Technical University of Denmark, Denmark
[c] Department of Logistics & Information Engineering, Tokyo University of Marine Science and Technology, Japan

ARTICLE INFO

Keywords:
Congestion pricing
Urban freight
Demand management
Traffic management
Simulation
Equity

ABSTRACT

The distributional impacts of congestion pricing have been widely discussed in the literature and the evidence on this is mixed. Some studies find that pricing is regressive whereas others suggest that it can be progressive or neutral depending on the specific spatial characteristics of the urban region, existing activity and travel patterns, and the design of the pricing scheme. Moreover, the welfare and distributional impacts of pricing have largely been studied in the context of passenger travel whereas freight has received relatively less attention. In this paper, we examine the impacts of several congestion pricing schemes on both passenger transport and freight in an integrated manner using a large-scale microsimulator (SimMobility) that explicitly simulates the behavioral decisions of the entire population of individuals and business establishments, dynamic multimodal network performance, and their interactions. Through simulations of a prototypical North American city, we find that a distance-based pricing scheme yields larger welfare gains than an area-based scheme, although the gains are a modest fraction of toll revenues (around 30%). In the absence of revenue recycling or redistribution, distance-based and cordon-based schemes are found to be particularly regressive. On average, lower income individuals lose as a result of the scheme, whereas higher income individuals gain. A similar trend is observed in the context of shippers — small establishments having lower shipment values lose on average whereas larger establishments with higher shipment values gain. We perform a detailed spatial analysis of distributional outcomes, and examine the impacts on network performance, activity generation, mode and departure time choices, and logistics operations.

1. Introduction

In 2018, transportation accounted for around 24% of global energy-related carbon dioxide emissions, with road transportation contributing three-quarters of this amount,[1] and in the United States in 2020, transportation accounted for 27% of anthropogenic greenhouse gas emissions.[2] Currently, 50% of the world's population resides in urban areas, and the rapid rate of urbanization on

* Corresponding author.
E-mail address: ravse@dtu.dk (R. Seshadri).

[1] https://ourworldindata.org/co2-emissions-from-transport.
[2] https://www.epa.gov/greenvehicles/fast-facts-transportation-greenhouse-gas-emissions.

https://doi.org/10.1016/j.tra.2024.104118
Received 10 May 2023; Received in revised form 22 December 2023; Accepted 22 May 2024
Available online 24 June 2024

a global scale has led to an increased demand for urban transportation. This proportion is expected to grow to 70% by 2050,[3] and consequently, competition for road surface area will likely remain stiff in the ensuing decades.

Cities are now, more than ever, contending with growing congestion and its consequences. In 2014 alone, U.S. auto commuters together lost an estimated 6.9 billion hours and 3.1 billion gallons of fuel to congestion — 42 h and 19 gallons wasted per commuter (Schrank et al., 2015). The global urban average in 2017 was not much better: 27 h and 13 gallons per driver (Cookson and Pishue, 2017). The rapid worldwide growth of on-demand mobility has also contributed to congestion. In the U.S., on-demand mobility has grown steadily, and its rise has led to the cannibalization of mass transit ridership by 6% from 2014 through 2016 (Circella and Alemi, 2018). Similar downward trends in mass transit ridership have been observed on a global scale.[4] E-commerce has also grown in significance over the past decade. A greater number of deliveries are made to consumers, driving the demand for urban freight. In addition to competing for existing road capacity, carriers make multiple stops along their routes, and depending on the nature of substitution and complementarity effects, this could exacerbate congestion and pollution.

The growing consensus is that demand management solutions are the most viable strategies to mitigate congestion whereas supply-oriented solutions (typically driven by road capacity expansion) are often less attractive and feasible, owing to their high costs and low impact (Gu et al., 2018). In particular, congestion pricing schemes – the standard economic prescription to internalize costs of negative externalities – are advantageous in that they encourage travelers to adjust all facets of their behavior including trip making, mode, departure-time and destination choices, as well as residential and work location (De Palma and Lindsey, 2011). Notable examples of congestion pricing schemes in practice include the cities of Singapore, Stockholm, Gothenburg, Milan and London (termed Downtown Congestion pricing by Lehe (2019)), and High-Occupancy/Express/Managed Lane facilities in the United States. Broadly, these schemes can be classified into four categories: facility-based, cordon, zonal, and distance-based schemes (see De Palma and Lindsey (2011) for a more detailed taxonomy). Extensive reviews of congestion pricing may be found in De Palma and Lindsey (2011), Santos and Verhoef (2011) and Anas and Lindsey (2011).

The welfare and distributional effects of congestion pricing (more generally, road pricing) have been widely studied in the literature. While it is generally the case that congestion pricing will generate a net welfare gain, the efficiency gains can often be dwarfed by distributional impacts (Eliasson and Mattsson, 2006; Arnott et al., 1994). The regressivity of pricing is often the focal point of public and political resistance to congestion pricing (for a detailed discussion on the political calculus underlying congestion pricing we refer the reader to King et al. (2007) and for more on equity and the different notions of progressivity, see Arnott et al. (1994) and Levinson (2010)). Nevertheless, the consensus from the literature on this is mixed. Several researchers have argued that congestion pricing is regressive in that prior to a redistribution of revenues, individuals with a high income and a higher value of time fare better than those with lower values (Anas, 2020; Anas and Hiramatsu, 2013; Arnott et al., 1994; Seshadri et al., 2022). Individuals with smaller economic margins generally have less flexibility in avoiding the toll charges (for example, by changing departure time), are more likely to live far from the city center and have destinations in areas where public transport is relatively poor (Eliasson and Mattsson, 2006). In contrast, and often in the context of European cities with better developed transit systems, researchers have found that pricing can be progressive (Eliasson and Mattsson, 2006; Santos and Rojey, 2004). Ultimately, the question of distributional impacts of pricing is likely to depend on the spatial structure of the city in question, socioeconomic characteristics and differences, and their relationship with activity and travel patterns, the design of the charging scheme, and so on (see Eliasson and Mattsson (2006) and Santos and Rojey (2004)). Moreover, assessing the performance of pricing schemes in general networks is complicated by network topology and the interdependence of flows, and discrepancies in findings from simple versus complex models in the literature point to the difficulty in drawing general conclusions (De Palma and Lindsey, 2011).

The aforementioned considerations motivate the need for evaluating the performance of congestion pricing schemes using large-scale disaggregate microsimulation models. Further, the increasing role of freight and e-commerce in urban congestion underscores the importance of examining the impacts on both passenger transport and freight. In this regard, this paper contributes to the literature in the following respects: (a) we propose an approach for the synthesis of business establishments for freight microsimulation models using publicly available data and apply the approach to generate a population of synthetic business establishments for Boston, (b) we comprehensively evaluate the impact of several congestion pricing schemes (area, distance, cordon) using an integrated passenger and freight agent-based microsimulation model of a large-scale prototypical North American city (involving a population of 4.6 million individuals and 0.130 million business establishments), and (c) we analyze welfare and distributional impacts on passengers and shippers, network performance impacts, impacts on activity patterns, and the effect on logistics operations.

It should be pointed out that our approach contrasts with those that utilize aggregate general equilibrium models (for example, the RELU-TRAN model of Anas and Liu (2007)) in that we focus exclusively on the transportation system (at a finer level of disaggregation). The general equilibrium approaches (e.g., Anas and Hiramatsu (2013), Anas (2020) and Anas and Chang (2023)) offer a more complete description of the system considering labor, housing and real-estate, production and travel markets simultaneously and hence, are appropriate when examining broader impacts of pricing on non-travel markets, land-use and real-estate, and for example, when examining revenue recycling measures such as cutting distortionary taxes. Our approach involves a more detailed model of travel-related decision making (including activity generation, mode, route, destination and departure-time choices) and dynamic network congestion, allowing for a detailed examination of the distributional outcomes in terms of accessibility.

To the best of our knowledge, our study is the first to examine the impacts of congestion pricing on both passenger and freight in an integrated manner using a large-scale microsimulation model that explicitly simulates the behavioral decisions of the entire population of individuals and business establishments, dynamic multimodal network performance, and their interactions.

[3] United Nations (2018). World Urbanization Prospects. https://population.un.org/wup/.

[4] UITP, (2017). Urban Public Transport in the 21st Century: Statistics Brief. https://bit.ly/2SihK9A.

2. Review of literature

The literature on congestion pricing is vast and includes the design and assessment of pricing using dynamic bottleneck models (Arnott et al., 1990, 1994; Van Den Berg and Verhoef, 2011a,b; Verhoef et al., 1996; Verhoef and Small, 2004), design of first-best pricing in general networks (Yang and Huang, 1998; Yang, 1999), design of second-best pricing schemes in general networks (Verhoef, 2002; Zhang and Yang, 2004), empirical assessments of congestion pricing using aggregate general equilibrium models (Anas and Hiramatsu, 2013; Anas, 2020) and large-scale static and dynamic network models (Eliasson and Mattsson, 2006; Eliasson, 2016; De Palma et al., 2005; Santos and Rojey, 2004). We restrict our attention to two streams of research, namely the study of congestion pricing using large-scale dynamic simulators and the impacts of pricing on freight. We refer the reader to the Santos and Verhoef (2011) and De Palma and Lindsey (2011) for more detailed reviews.

2.1. Impacts of pricing using large-scale static and dynamic simulators

There exist several large-scale agent-based simulation models that have been developed over the years. These include MATSim (W. Axhausen et al., 2016), POLARIS (Auld et al., 2016), SimMobility (Oh et al., 2021; Adnan et al., 2016), METROPOLIS (De Palma et al., 1997), etc. However, detailed quantitative assessments of congestion pricing using such models is surprisingly sparse.

De Palma et al. (2005) analyzes several link-based road pricing schemes using the dynamic network simulator METROPOLIS, which endogenously models departure time, route and mode choice decisions. Using a stylized urban road network consisting of radial arterials and circumferential ring roads, they find that step tolls outperform flat tolls and generate smaller revenues, leading to more favorable distributional outcomes.

Several studies have used the multi-agent simulation platform MATSim to examine the impacts of congestion pricing schemes in different contexts. Kaddoura and Nagel (2019) examines the impacts of two pricing schemes, based on marginal external congestion costs and a control-theoretical approach. They perform experiments by simulating 10% of the population of the Greater Berlin region with appropriately reduced link capacities. The findings suggest that the pricing policies cannot completely eliminate queuing and that the overall welfare gains are between 2.5% and 14% of toll revenues. Simoni et al. (2019) examines the impacts of several congestion pricing schemes for future scenarios with automated and shared automated vehicles. They employ agent-based simulations of the city of Austin and its surroundings (once again, they simulate a fraction of the population, in this case 5%), and find that a travel time-congestion-based scheme yields the highest welfare gains. Finally, more recently, He et al. (2021) study the impacts of pricing schemes in New York City using a calibrated NYC MATSim model. They use a 4% sample of the population (around 320 000) for simulation. In contrast with most previous studies, they find a net increase in consumer surplus prior to any redistribution of toll revenues and attribute this to heterogeneity in values of time.

Lentzakis et al. (2020) and Lentzakis et al. (2023) demonstrate the superiority of distance-based congestion pricing schemes (in terms of overall welfare gains) over area- and cordon-based schemes using simulations of the network of Singapore expressways and downtown Boston. They employ the real-time Dynamic Traffic Assignment model system DynaMIT2.0 (Zhang et al., 2017, 2021) considering departure time and route choices under elastic demand.

Finally, several studies have employed aggregate general equilibrium models to examine the broader impacts of congestion pricing on the urban economy. Anas (2020), through an application of the RELU-TRAN model (Anas and Liu, 2007) to the LA region, concluded that the aggregate benefit of pricing road congestion increases significantly when the toll revenue is recycled to cut the income tax of poorer workers (while maintaining region-wide tax revenue neutrality). Moreover, the impacts on urban markets are relatively small owing to the high elasticities of substitution between routes. Anas and Hiramatsu (2013), using the RELU-TRAN model applied to Chicago, found that an optimal cordon pricing policy can achieve up to 65% of the gains from Pigouvian tolling (a large portion of which come from increases in real-estate values) and importantly, broad outer cordons have the effect of centralizing economic activity, jobs and residences.

2.2. Impacts of pricing on freight

The impact of pricing on freight demand has not been studied as much as that on passenger demand. Waliszewski (2005) surveyed the potential impacts of congestion pricing on urban freight based on available data. Although London's congestion charging scheme resulted in a reduction in the number of trucks, the proportion of trucks among all road traffic increased. This could be due to the interaction of a number of factors including differences in demand elasticity, changes to shipment frequency, stops per tour and effects of non-travel markets. The cases in New York City, Switzerland, and Austria suggest that tolling trucks for externalities would lead to more equitable and efficient truck operations. In Switzerland and many European cities where distance-based charging is implemented for trucks, evidence suggests that long-distance travel becomes less efficient and frequent. Holguín-Veras et al. (2006) assessed a time-of-day pricing initiative on commercial carriers for toll facilities operated by the Port Authority of New York and New Jersey. The authors note that the carrier responses to the pricing are complex and heterogeneous, involving changes in toll facility usage, productivity increases, and cost transfers to the end consumer. They indicated that the constraints that prevent carriers from changing operations from peak-hours to non-peak-hours are significant. Holguín-Veras (2010) corroborated this, concluding that freight mode choice and delivery time choice are jointly made by shippers and carriers, so carrier-centered pricing schemes may not always achieve the desired impacts. Furthermore, Holguín-Veras (2011) modeled the cost transfer between carriers and receivers and derived theoretical impacts of cordon pricing, time – distance pricing, and carrier – receiver policies on the urban

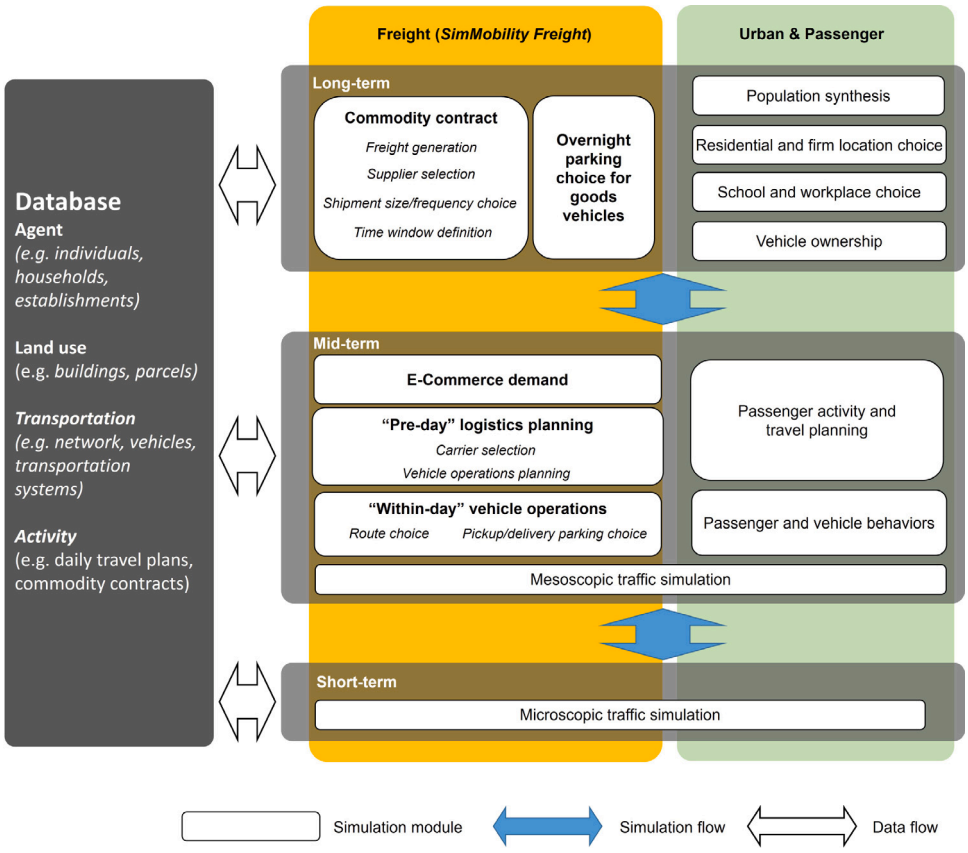

Fig. 1. SimMobility framework.

delivery industry in competitive markets. The results suggest that cordon time-of-day pricing cannot transfer costs to receivers and is thus ineffective, whereas time-distance pricing could transfer costs to receivers with huge unit tolls.

Chen et al. (2018) developed a transportation network equilibrium model and quantified the temporal shift of freight traffic under congestion pricing. They use a simple network with two origins and one destination. The results highlight that, with increasing VOT, the equilibrium flows decrease and the average speed increases, indicating better effectiveness in congestion reduction and network throughput. Although VOT is the key consideration in decision-making and measuring cost sensitivity, Chen et al. (2018) assume a single VOT for each simulation. Finally, to understand the heterogeneity among drivers, Toledo et al. (2020) develop a mixed logit model with a path-size factor for truck driver route choices, incorporating heterogeneity by employment term and vehicle characteristics.

In summary, to the best of our knowledge, there are no integrated quantitative assessments of congestion pricing on both passenger transport and freight, the impacts on freight have been less studied, and moreover, applications of large-scale agent-based simulators have tended to use a small fraction of the population for simulation, which may or may not accurately capture system-wide impacts.

3. Agent-based microsimulation model

In assessing the impacts of congestion pricing schemes, it is imperative that in addition to overall welfare gains, distributional impacts are reliably quantified and 'winners' and 'losers' from the policy are identified. Equity issues associated with congestion pricing have long been recognized (Levinson, 2010) and mitigating the regressive effects of pricing remain the key to ensuring public acceptability. This motivates the need for a disaggregate microsimulation-based approach that explicitly models the behavior of individual passenger and freight agents. For this, we utilize an open-source agent-based passenger and freight microsimulator, SimMobility (Adnan et al., 2016). In this section, we provide a concise description of SimMobility and detail enhancements on the freight side to model price sensitivity.

3.1. Overview

SimMobility simulates agents' behavioral decisions at three different temporal scales — long-term, mid-term, and short-term (Fig. 1). The long-term model simulates strategic decisions involving time periods longer than a day (e.g., residential locations,

business locations, and commodity contracts). On the passenger side, agents are individuals and households whereas on the freight side, each establishment is an agent, and can play the role of a shipper, a carrier, a receiver, or a combination of these. The long-term model includes population synthesis, the simulation of residential, school, workplace, business location choice, and vehicle ownership for passengers and business establishments. A business establishment also decides on commodity contracts (that determine business-to-business (B2B) commodity flows between establishments) and chooses overnight parking locations of freight vehicles. Here, a commodity contract defines the origin and destination of a commodity flow, commodity type, contract size, shipment size and frequency.

The mid-term model simulates individuals' activities and freight deliveries at the day level. The mid-term model combines activity-travel based demand models with multimodal dynamic, mesoscopic network assignment. The demand simulator comprises two groups of behavior models: pre-day and within-day. The *pre-day* models simulate the plans of all the individuals and freight-related establishments, as well as e-commerce orders, while within-day models adapt these plans based on the current network conditions and constraints. The *Supply* module then simulates the movement of individuals and vehicles (mass transit, on-demand, and freight) and their interactions based on a combination of macroscopic speed-density relationships and queueing models. The decisions of supply agents such as public transit and on-demand service operators are explicitly modeled (Oh et al., 2020).

Finally, the short-term model is a microsimulator of transportation operations with high temporal resolution including models of car-following and lane-changing. The simulation time step is typically a fraction of a second. Note that for the simulations in this paper, we do not make use of either the long-term passenger model or the short-term model. In other words, long-term residential and workplace location choices are not modeled and are exogenous.

3.2. Passenger demand

The pre-day passenger demand module is an activity-based model system that adopts the day-activity schedule approach (Bowman and Ben-Akiva, 2001). It predicts an activity-travel schedule (plan) for each individual in the population including the number and types of activities performed, their duration and time-of-day, locations, and travel modes. As shown in Fig. 10 in Appendix A, it is a system of hierarchical discrete choice models (logit and nested-logit) organized into three levels: the day-pattern level, the tour level and the intermediate stop level. Bottom-level decisions are conditional on upper-level decisions and the levels are related through 'logsums' or 'inclusive values' (expected maximum utility) indicated by dashed lines. The inclusive values capture the sensitivity of activity and travel decisions modeled at the higher levels of the hierarchy to the utility associated with conditional outcomes from the lower level models. All the stop and tour-level models are sensitive to pricing and consequently, so are the upper-level day pattern decisions through the logsums.

For work and education activities that have a fixed location, the choice of mode is modeled through tour mode choice models (using logit models with heterogeneity in the value-of-time) with individual specific choice-sets that account for vehicle ownership, transit availability and distance thresholds for walking and bicycling. The variables include attributes such as travel time components (in-vehicle, access/egress, waiting), transfers in public transit, monetary cost, vehicle ownership, and socio-demographic dummies (age, gender, education, and income). For activities which involve a destination choice (shopping, recreation, escort, personal, work with non fixed location), the choice of mode and destination is modeled jointly. We use logit models with heterogeneous value-of-time, which include the complete choice set of mode-destination combinations. The variables include mode-specific travel time components, monetary costs, and 'size' variables for each destination zone such as area, employment, population and a dummy for the central business district. These 'size' variables are incorporated using the aggregate spatial method outlined in Ben-Akiva and Watanatada (1981). Finally, the time-of-day models determine the start and end time of the primary activities. The 24 h day is discretized into 48 half-hour segments and the choice set includes all feasible combinations of start and end segment, leading to 1176 alternatives. The alternative specific constants in the model follow a continuous and cyclical form using a trignometric functional form (described in Ben-Akiva and Abou-Zeid (2013)). The variables include travel times, costs, and activity duration. More details on the specification and calibration of the models are provided in Section 4.

The within-day module transforms the pre-day plans into actions and includes path-size logit models of private and public route choice. The attributes in the private route choice model includes travel time, toll cost, distance, number of signalized intersections, and number of right turns. The attributes in the public-transit route choice model includes in-vehicle time, wait-time, walk-time, and number of transfers. We refer the reader to Adnan et al. (2016) and Tan et al. (2015) for more details on the structure of the route choice models.

3.3. Freight demand

A detailed description of the structure of the freight demand models may be found in Sakai et al. (2020b). In the long-term, establishments (either as receivers or shippers or both) generate demands for B2B commodity flows through freight generation (production and consumption), supplier selection, and shipment size and frequency selection. At the mid-term pre-day level, households and e-commerce vendors (as shippers) generate B2C shipments, shipper establishments select carrier establishments, and finally, carriers plan their vehicle operations. The process of assigning shipments to vehicles and developing vehicle tours is called vehicle operations planning (VOP). At the mid-term within-day level, freight vehicle drivers make route and parking choices considering real-time traffic information. In the decision-making of establishments (and their drivers) and households, we assume they are independent entities that make decisions individually. Admittedly, this is a simplistic assumption and one we make due to limited knowledge about their interactions. The key models (at the long-term and mid-term level) sensitive to congestion pricing

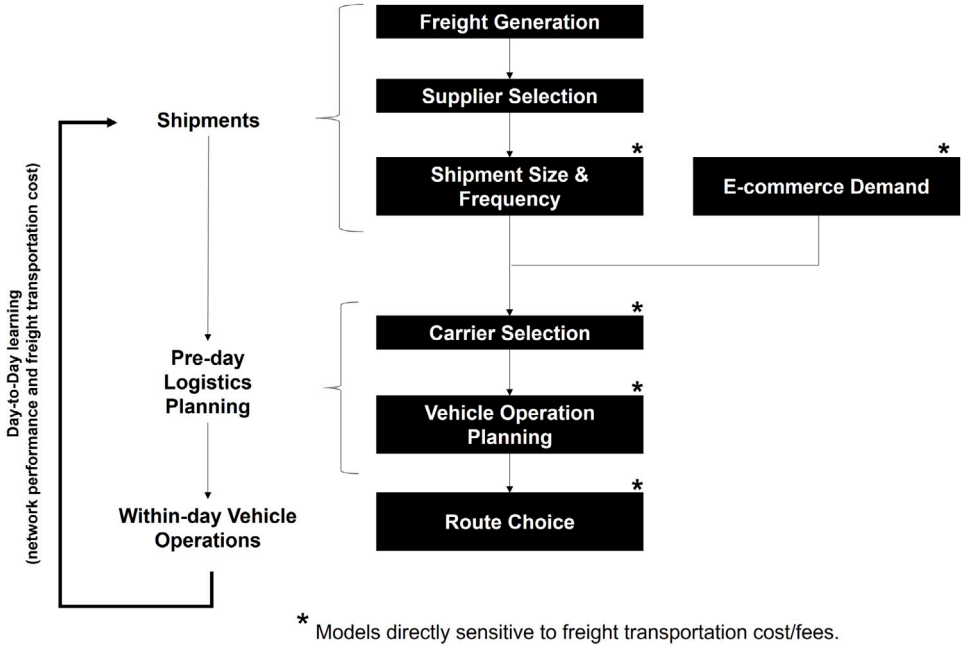

Fig. 2. Price sensitive models in SimMobility freight.

are summarized in Fig. 2. We assume that overall freight generation is not affected considering that city-level pricing schemes have negligible impact on regional or global B2B commodity production and consumption, whereas shippers' shipment size and frequency decisions, and e-commerce demand are affected. Carriers are also sensitive to costs in VOP. In the within-day level, the drivers' route choice is sensitive to toll costs. A detailed description of the models and enhancements to incorporate price sensitivity are provided next. Details on the estimation and calibration of model parameters are provided in Section 4.

3.3.1. Shipment size and frequency

The shipment size and frequency model is an enhanced version of the model in Sakai et al. (2020b). It determines the shipment sizes and frequencies in commodity contracts. The model relies on economic order quantity theory. A shipper s optimizes the shipment size to minimize the annual logistics cost of a contract, where three cost components are relevant to the quantity. The total logistics cost (TLC) for a contract i is defined as:

$$TLC_i = T_i + I_i + K_i, \tag{1}$$

where I_i is the inventory cost incurred by receiver r, K_i is the capital cost during transportation, and T_i is the transportation cost incurred by the receiver. It should be noted that other components such as cost of deterioration and damage during transport, capital cost during transport, and stockout cost, are not included because they are not functions of shipment size and do not affect the shipment size selection. For simplicity, the subscript i is omitted in following discussion. The inventory cost is assumed to be:

$$I = w_{s,r}^{com} \times q/2, \tag{2}$$

where $w_{s,r}^{com}$ is the commodity type and location specific inventory cost per weight unit, and q is the shipment size by weight. $w_{s,r}^{com}$ is assumed to be linear in the establishment density at the receiver's location:

$$w_{s,r}^{com} = \beta_{ED}^{com} \times ED_r, \tag{3}$$

where ED_r is the establishment density at the receiver location and β_{ED}^{com} is a unknown parameter. The capital cost is:

$$K = d \times v^{com} \times q/2, \tag{4}$$

where d is the discount rate, v^{com} is the commodity-type-specific goods value per unit of weight. Finally, transport cost is given by:

$$T = (Q/q) \times o_{s,r}^{com}, \tag{5}$$

where Q is the annual commodity flow by weight, $o_{s,r}^{com}$ is the commodity type and OD specific transport cost. We define $o_{s,r}^{com}$ as a function of average operation costs (including tolls):

$$o_{s,r}^{com} = \left(\beta_{q_0}^{com} + \beta_q^{com} q\right) \times AOC_{s,r}^{com}, \tag{6}$$

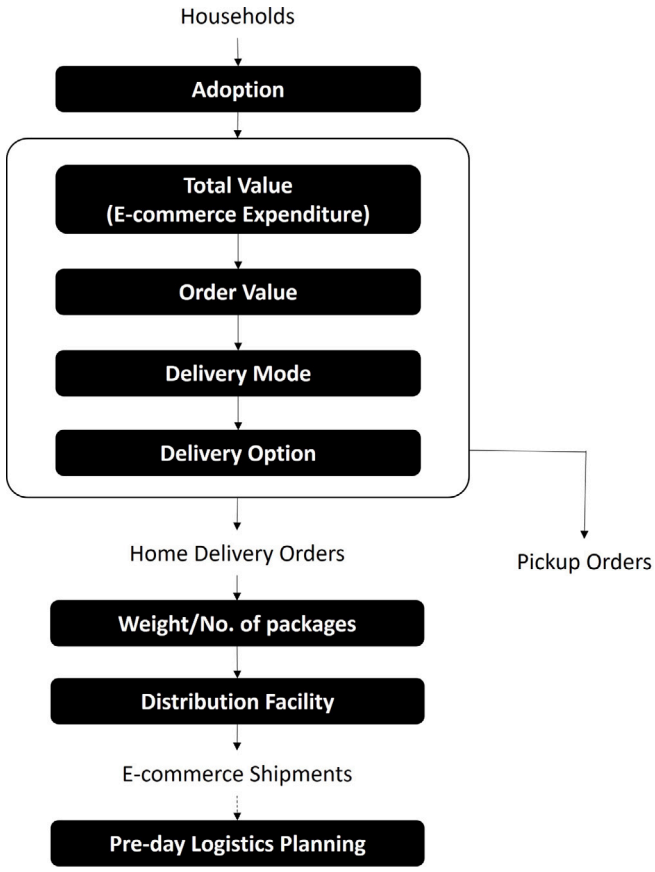

Fig. 3. Flow of household-based E-commerce demand simulation.
Source: Modified from Sakai et al. (2022).

where $AOC_{s,r}^{com}$ is calculated as the total operation cost divided by the total number of shipments for each combination of OD and commodity type, and is updated iteratively within the day-to-day learning process described in Section 3.4. $\beta_{q_0}^{com}$ and β_{q}^{com} are unknown parameters (more details are provided in Section 5). Note that we make some simplifying assumptions when defining operating costs (see Hummels (1999) and De Jong and Ben-Akiva (2007) for a more detailed discussion). From the above equations, the optimal shipment size is given by:

$$q = \left(\frac{2 \times \beta_{q_0}^{com} \times Q \times AOC_{s,r}^{com}}{\beta_{ED}^{com} \times ED_r + d \times v^{com}} \right)^{0.5}, \tag{7}$$

where $\beta_{q_0}^{com}$ and β_{ED}^{com} are model parameters. With congestion pricing, if $AOC_{s,r}^{com}$ increases, then the shipment size increases. It is expected that the size change would be more significant for contracts that have lower commodity value and for ODs with higher cost. Note that since the calibration of only $\beta_{q_0}^{com}$ and β_{ED}^{com} in Eq. (7) cannot reproduce the observed shipment size distribution (this issue is pointed also by Sakai et al. (2020a) using the data from Tokyo, Japan), we introduce an additional parameter β_Q:

$$q = \left(\frac{2 \times \beta_{q_0}^{com} \times Q^{\beta_Q} \times AOC_{s,r}^{com}}{\beta_{ED}^{com} \times ED_r + d \times v^{com}} \right)^{0.5}. \tag{8}$$

3.3.2. E-commerce demand

In the e-commerce demand model, each household is considered the decision-maker, which makes orders (or purchase decisions) relating to three commodity types: groceries, household goods, other durable goods. The model is a hierarchical set of discrete choice models (Fig. 3). The details of the each step of the household-based e-commerce model are available in Sakai et al. (2022).

We assume that delivery fees to households within a tolled region will increase, although fees for the pickup option will remain the same. Although shippers might not be affected by congestion pricing or even benefit from it, we assume that they will still attempt to transfer the toll cost to receivers and apply an increase in delivery fees by a rate equal to the total amount of toll paid by freight vehicles divided by the number of deliveries within the toll area (including e-commerce and non-e-commerce shipments).

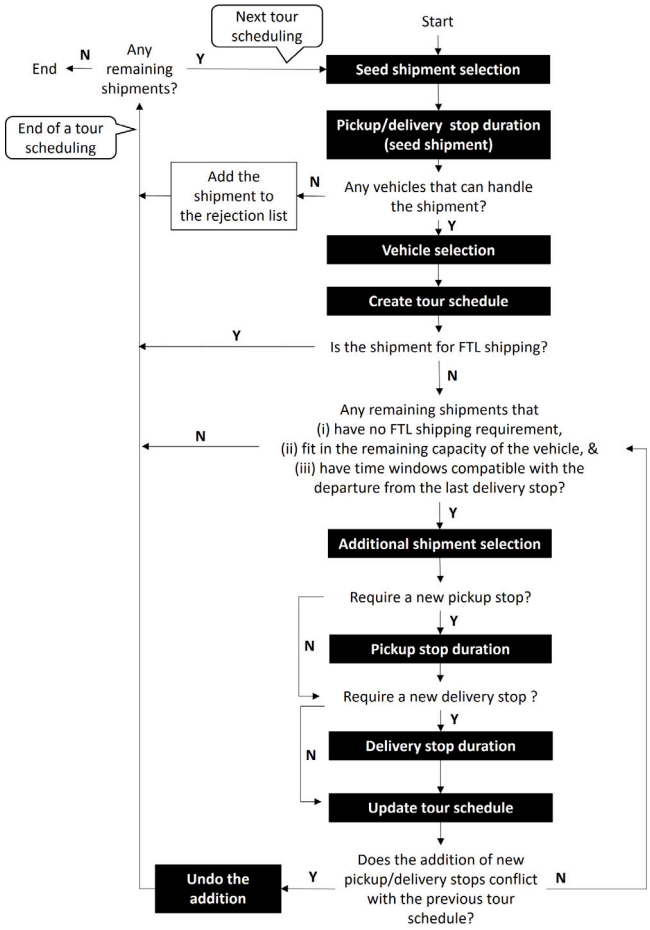

Fig. 4. Flow of vehicle operations planning.
Source: Modified from Sakai et al. (2020b).

3.3.3. Vehicle operations planning

The decision-makers of VOP are freight carriers. Under feasibility constraints, they make decisions on shipment-to-vehicle assignment and fleet tour schedules. The model inputs are carriers, carriers' fleets (payload capacity and body type), shipments assigned to carriers (pickup and delivery locations, delivery time window, size, and shipping requirement (parcel, full truckload, or less than truckload)), and network information. The flow of VOP proposed by Sakai et al. (2020b) is shown in Fig. 4. The heuristic assigns shipments, one-by-one, to carrier's goods vehicles and generates vehicle tours for pickups and deliveries.

The limitation of the heuristic proposed in Sakai et al. (2020b) is that the model is not sensitive to tolls, though it is sensitive to travel time. Therefore, we develop a logit model to enhance the VOP heuristic, assuming the decision rule is utility maximization under feasibility constraints. Note that we use the term utility out of convenience, shippers in fact maximize profits. For a carrier n, the systematic part of the utility function of a VOP alternative i is:

$$\begin{aligned} V_{ni} = & \sum_{v \in fleet_n} \sum_{t \in trips_{i,v}} -toll_t + \beta_1 \times time_t + \\ & (\beta_2 \times \delta_{LGV_t} + \beta_3 \times \delta_{HGV_t} + \\ & \beta_4 \times \delta_{VHGV_t}) \times distance_t, \end{aligned} \tag{9}$$

where $fleet_n$ is the set of candidate freight vehicles belonging to the carrier n, v is a freight vehicle of carrier, t is a trip made by the vehicle, and $trips_{i,v}$ is the set of trips made by vehicle v under alternative i. The utility function takes a money-metric form. We include toll ($toll_t$), total time ($time_t$), and distance ($distance_t$) as cost-related variables for trip t. Total time (including travel and dwell time at pickup and delivery stops) is used as a proxy of driver wage. We make this simple assumption because most urban freight drivers are paid by the hour, which is the most common form of payment for urban and LGV drivers. Along the lines of Perera (2019), distance interacted with vehicle body type dummies (δ_{LGV_t}, δ_{HGV_t}, δ_{VHGV_t}) serve as proxies for vehicle-based costs (fuel, tire, repair, maintenance, and depreciation). Carriers use travel time, distance, and toll information based on their experience

from the day-to-day learning process (refer Section 3.4). The travel time, distance, and toll represent values from the trip origin zone to the trip destination zone by departure time (AM peak, PM peak, or off peak). All trips of all vehicles, including returning to overnight parking locations, are included in the cost calculation. In addition, utilizing the concept of the path-size variable in route choice (Ramming, 2001), we define an overlap factor (denoted OF) to penalize the overlap between alternative plans (see Appendix C for details).

The utility function for carrier n and VOP alternative i is the sum of the systematic part, the overlap factor, and the error term, which follows an extreme value distribution with scale parameter μ:

$$U_{ni} = V_{ni} + \beta_5 \times \log(OF_{ni}) + \epsilon_{ni}/\mu, \tag{10}$$

In the choice set generation process, a set of feasible alternative vehicle operations plans are generated. We use several alternative criteria to order the shipments and vehicles in the *seed shipment selection*, *vehicle selection*, and *additional shipment selection* modules in Fig. 4.

3.3.4. Route choice

The route-choice model for freight carriers is described in detail in Toledo et al. (2020).

3.4. Supply

The pre-day and within-day passenger and freight models yield trip-chains for each individual and vehicle tours for each freight vehicle, which are simulated on a multimodal network using the Supply module, which is a mesoscopic traffic simulator. The Supply module includes bus and rail controllers to manage public transit operations including the frequency/headway-based dispatching of vehicles, monitoring of occupancy, dwelling at stops and so on. More details may be found in Lu et al. (2015) and Oh et al. (2020). Finally, demand–supply interactions are explicitly modeled through the iterative day-to-day and within-day learning processes, which involve a successive averaging of time-dependent zone-to-zone and link-level travel times respectively, until an acceptable measure of convergence between travel times in successive iterations is achieved. However, given computational constraints, the number of day-to-day iterations we perform is limited and hence, our framework can be considered a pseudo-equilibrium approach.

4. Prototype city generation and calibration

The study area is a prototype city representing a typology or class of cities termed *Auto-Innovative* (Oke et al., 2019). This type of city is characterized by modernization and industrialization, high auto-dependency, and high transit mode share, as well as high metro and population density, mainly representing North American cities (e.g., Boston, Washington D.C., Chicago, Toronto). The prototype city is synthesized based on population, land use, and supply characteristics of the Greater Boston Area (GBA), which serves as an archetype city — one that is close to typology averages on many indicators. The key characteristics of the city are as follows:

- Zoning: 164 municipalities, 2727 traffic analysis zones (TAZs)
- Area: 7.32 thousand square kilometers
- Road network: 18 016 nodes and 46 763 links
- Population: 1.74 million households, 4.60 million residents
- Business establishments: 0.130 million
- Vehicles: 2.47 million passenger vehicles, 0.378 million goods vehicles

The pre-day activity-based models were originally estimated from the 2010 Massachusetts Travel Survey data and time and cost skim matrices from Boston's Central Transportation Planning Staff. Model specification details are described in Viegas de Lima et al. (2018). These models were then calibrated to ensure that demand and activity patterns match typology averages as described in Oke et al. (2020).

Further, to better represent heterogeneity in travelers, we introduced lognormally distributed (see Hess et al. (2005)) values of time (VOT) to the time-of-day and mode-destination choice models, where individuals from higher income groups are assumed to have a higher VOT. The mean-values of the parameters associated with the cost variables were calibrated to ensure that the aggregate cost elasticities (Table 1) accord with empirical values indicated in the literature (mode choice: Vega and Reynolds-Feighan (2008), Bhat (2000) and Yang et al. (2013); time-of-day choice: Ding et al. (2015), Sasic and Habib (2013) and Bhat (1998)). For more details on the calibration of the standard deviation of the randomly distributed cost co-efficients, refer the reader to Chapter 2 of Jing (2022) (the literature reports a ranges of values, see Seshadri et al. (2022)).

The prototype city generation described in Oke et al. (2020) considers the passenger side only. In order to model freight, we augmented this synthetic prototype city by synthesizing business establishments (described in the supplementary material). Using the synthesized establishments, we calibrated the long-term model parameters, which determine B2B commodity flows. The initial long-term model parameters were estimated using data from the 2013 Tokyo Metropolitan Freight Survey. We re-calibrated them based on a Public Use Microdata (PUM) from the 2012 Commodity Flow Survey (CFS) (U.S. Census Bureau, 2012), which contains shipment records including origin, destination, size, commodity type, and shipper industry type. The samples in PUM are mainly manufactures and wholesalers. We also used the aggregate commodity OD flows from Freight Analysis Framework (FAF4) data to complement to PUM for other industry types. We introduced adjustment factors for production model parameters so that, for

Table 1
Aggregate cost elasticity in passenger models.

Model	Level	Alternative	Activity type	Elasticity
Mode-destination choice	Tour	Car	Work Education Shop Other	−0.082 −0.20 −0.21 −0.23
Mode choice	Tour	Car	Work Education	−0.10 −0.18
Mode choice Mode choice	Sub-tour Intermediate stop	Car Car	Work Any	−0.13 −0.18
Time of day	Tour	Depart during AM or PM peak using car	Work Education Shop/Other	−0.11 −0.15 −0.23
Time of day	Sub-tour	Depart during AM peak using car Depart during PM peak using car Depart during off peak using car	Work	−0.14 −0.16 −0.21
Time of day	Intermediate stop	Depart during AM peak using car Depart during PM peak using car Depart during off peak using car	Any	−0.18 −0.19 −0.23

Table 2
Parameter values in the VOP model.

Parameter	Value	Sources
β_1	−27.32	Hourly driver wage and benefit in Murray and Glidewell (2020); cross-validated with Massachusetts average delivery driver wage
β_2 β_3 β_4	−0.57 −0.67 −0.72	Based on Murray and Glidewell (2020), fuel consumption rates adjusted to urban speed using National Institute for Land and Infrastructure Management (2016)
β_5 μ	1.61 1.18	Estimated values from truck route choice model with data from Ben-Akiva et al. (2016) with the same specification

manufacturers and wholesalers, the aggregated commodity production by industry and commodity type from the model correspond to those based on PUM. After this, we introduced adjustment factors for production and consumption model parameters (except those already adjusted) to match the aggregated simulated production and consumption (by commodity type) with those based on FAF4. Further, the shipment size model parameters (Eq. (8)) are also calibrated to match the cumulative distributions of simulated shipment size for manufacturing and wholesale industries with those from on PUM.

To calibrate e-commerce demand model, various types of datasets were used while it counted mainly on 2017 National Household Travel Survey (U.S. Federal Highway Administration) data, which include the count of times purchased online for delivery. The details of the calibration process are available in Sakai et al. (2022).

For setting the model parameters for the VOP model (βs and μ shown in Eqs. (9) and (10)), we used various sources (summarized in Table 2). We primarily use documents published by the American Trucking Research Institute (ATRI), which give factors for converting time and distance to itemized costs. However, over 80% of the vehicles studied by ATRI are intercity trucks operating at higher speeds than urban vehicles. Therefore, we used the speed to fuel consumption relationship of freight vehicles operating at lower speeds in urban areas (National Institute for Land and Infrastructure Management, 2016); we adjusted the distance-to-fuel-cost factors in the ATRI report (Murray and Glidewell, 2020) for the urban setting. Next, the coefficient of the overlap factor and the scale parameter are affected by the level of stochasticity in decision-making and are not easily found in literature. We used the truck driver survey data in North America conducted in 2012 (Ben-Akiva et al., 2016) to obtain the estimates for them as well as the route choice model parameters. The dataset and choice set generation process for the route choice model are detailed in Toledo et al. (2020), and the specification of the utility function used in SimMobility is available in Sakai et al. (2020b).

5. Design of congestion pricing schemes

5.1. Scenario design

We consider the following four scenarios: (a) baseline scenario or do-nothing (Base), (b) distance-based pricing (Distance): toll charge is proportional to the distance traveled within the tolled area with an upper limit for each vehicle during a day and the tariff is time-varying, (c) cordon-based pricing (Cordon): a vehicle is charged each time it enters the tolled area through radial road links (vehicles exiting the area are not tolled and the tariff is time-varying), (d) area-based pricing (Area): a vehicle traveling within the tolled area from the start of the AM peak to the end of the PM peak pays a flat toll charge during a day. Cordon tolls affect only inbound trips (inbound to the charging area on selected radial roads) in the peak period. The area-based scheme charges a flat fee for the entire day (including the afternoon off-peak period) for travel within the area (a vehicle that makes multiple trips within the

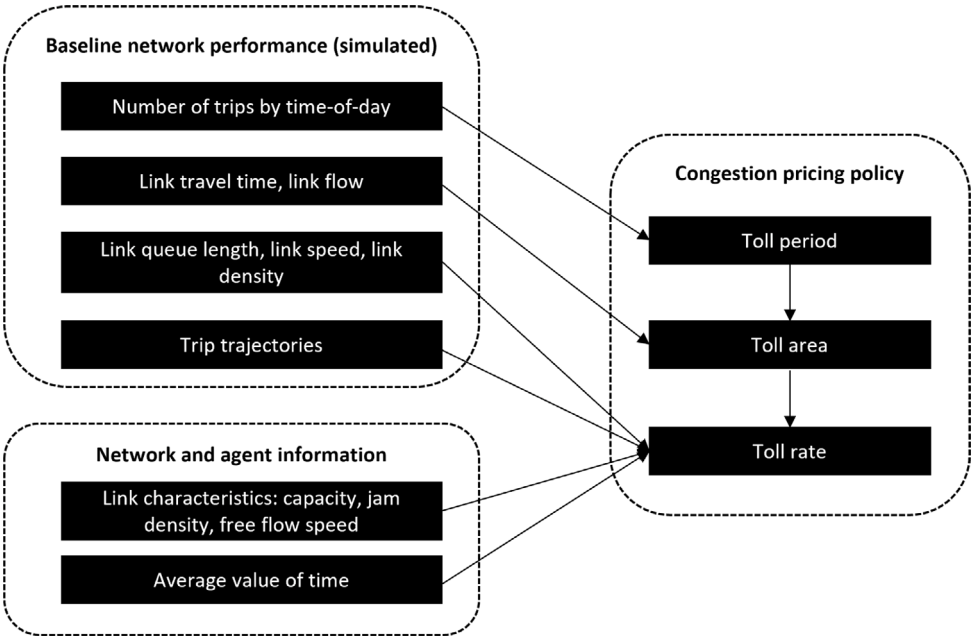

Fig. 5. Framework for congestion pricing policy design.

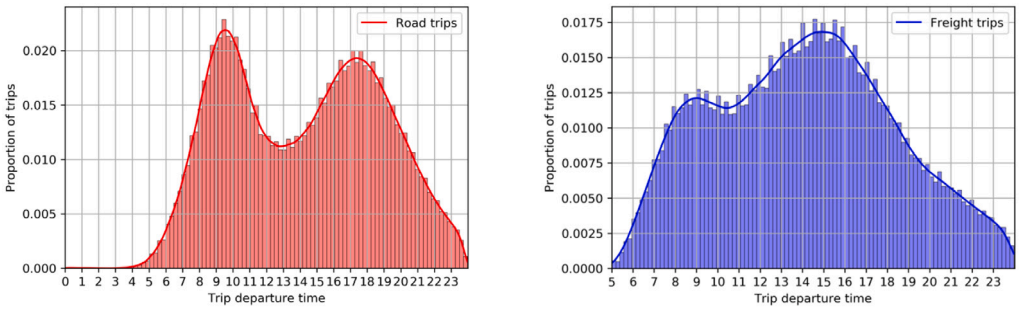

(a) Passenger car trips by time-of-day

(b) Freight trips by time-of-day

Fig. 6. Trip time-of-day patterns.

charging area pays the fee only once). Finally, in the distance-based scheme, vehicles pay a toll proportional to the total distance traveled in the peak periods subject to a cap (regardless of whether this distance occurs over multiple trips or a single trip).

The congestion pricing policies we examine share several features. First, they are *location-specific* in that tolls are applied for a specific area of the city consisting of several traffic analysis zones. Second, they are *time-period-specific* in that toll-rates are different during different periods of the day. Third, they are *vehicle-type* specific in that toll-rates are based on passenger-car-units of the vehicle. Based on the maximum laden weight, goods vehicles are classified as light goods vehicles (LGV) (no more than 3.5 ton), heavy goods vehicles (HGV) (3.5–16 ton), very heavy goods vehicles (VHGV) (more than 16 ton), of which the PCU is 1.5, 2, 2.5 respectively.

The overall framework adopted for the design of the pricing schemes is summarized in Fig. 5. The design utilizes information of network performance from a simulation of the baseline scenario along with agent-level information. We first examine the number of trips by time-of-day to identify the cities' peak hours and determine toll period(s) accordingly. Next, we quantify the extent of congestion during the tolling periods at the level of traffic analysis zones (TAZ) to define a tolling area for all three pricing schemes. Finally, we use simulated network performance information to approximately estimate congestion externalities of each link (and for all tolled vehicles using trajectories) by time-of-day.

5.2. Toll period

Fig. 6 shows the number of passenger car and freight trips by departure time on an average weekday from the calibrated model. Based on these, we define tolling periods (for the distance- and cordon-based schemes) between 8–10 AM (AM peak) and 4–7 PM

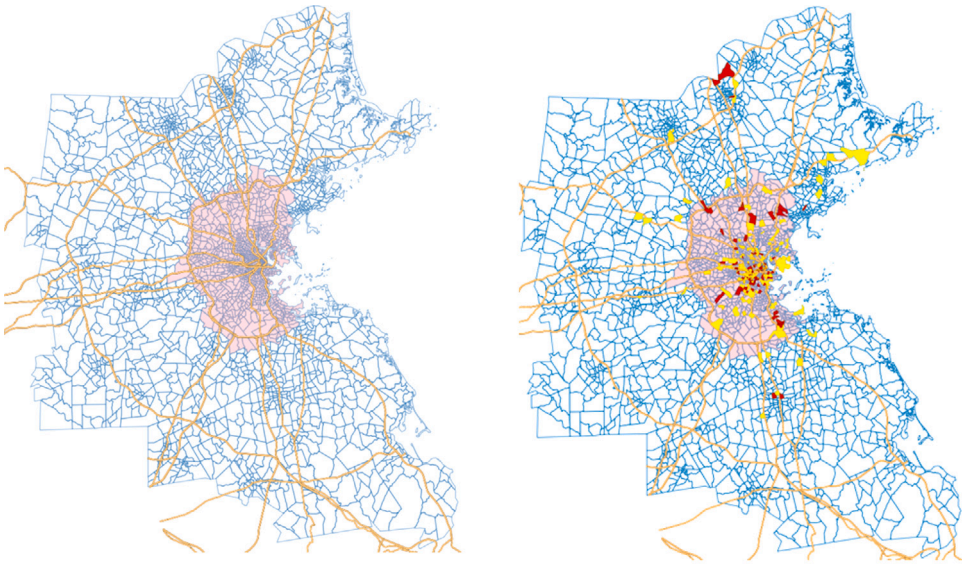

(a) Tolled area (b) TAZs with high TTI

Fig. 7. Tolled area in prototype city. (For interpretation of the references to color in this figure legend, the reader is referred to the web version of this article.)

(PM peak). Tolls are also applied during 30 min before and after the peak periods with lower rates, as ramp up/down periods to avoid abrupt changes in demand. It is worth-noting that the freight trips have significantly different patterns of departure time. However, given that the overall proportion of freight trips is small (~7%), we define the tolling periods largely based on passenger trip patterns.

5.3. Toll area

In order to define the toll area, we use the travel time index (TTI), which is the ratio congested travel time to free-flow travel time as an indicator of congestion. The link-flow weighted average TTI is computed across all links for each TAZ. Based on the computed TTI, we can identify an appropriate area or region to be tolled. There are several additional considerations based on judgment. The tolled area should cover as many congested TAZs as possible and natural barriers (e.g., rivers, coasts, freeways) may help define borders of the tolled region for ease of implementation.

As shown in Fig. 7(b), we find the TAZs with a relatively higher average TTI (1.2+) are highly concentrated in the eastern bay of the city (yellow indicates zones with a high TTI in the AM peak while red zones indicate a high TTI in the PM peak). We define the tolled area as the shaded area so it includes most of the those TAZs. The eastern boundary is the natural coastline and the western boundary of is a major freeway. The toll area spans over 791 square kilometers (10.8% of total area) and has 1.85 million residents (40.2% of total population) and 9652 business establishments (7.7% of total), which indicates that the population density is much higher than that of the entire city. The temporal and spatial patterns of trips in the Base scenario are summarized in Table 3, based on trip departure time and origin–destination (OD) pair. External trips have both ODs outside of the tolled area, internal trips have both ODs within the tolled area, and connection trips have the destination within the tolled area (entering) or origin within the tolled area (exiting).

5.4. Toll rates

In order to set the toll rates for each charging scheme, we approximately estimate the marginal external costs of congestion (i.e., the marginal cost tolls) using network performance measures from the baseline simulation. Within the mesoscopic supply model, each network segment consists of a moving part (where traffic dynamics are governed by a modified Greenshields model) and a queuing part (where vehicles incur deterministic queuing delays). For a given five-minute time interval, the marginal cost toll on a segment i, δ_i can be expressed as (see Lentzakis et al. (2020) and Yang and Huang (1998)):

$$\delta_i = \gamma q_i \left(\frac{dt_i}{dq_i} \right) + \gamma \left(\frac{n_i^q}{c_i} \right), \tag{11}$$

where γ is an average value of time of travelers traversing the segment in the five-minute interval in $ per hour, t_i is the average travel time on segment i, n_i^q is the average number of queuing vehicles, q_i is the flow in vehicles per hour during the five-minute interval and c_i is the segment capacity in vehicles per hour. The expression for the first term may be found in Lentzakis et al. (2020)

Table 3
Total trips: Passenger and freight.

Time-of-day	Trip type	Total	Internal	Entering	Exiting	External
All day	Passenger trips (million)	12.1	3.99	1.08	1.07	5.97
	% in passenger trips	100%	32.9%	8.9%	8.8%	49.3%
	Freight trips (million)	1.00	0.34	0.09	0.09	0.47
	% in freight trips	100%	34.1%	9.4%	9.3%	47.1%
AM peak	Passenger trips (million)	2.01	0.66	0.22	0.15	0.98
	% in passenger trips	100%	32.8%	11.1%	7.3%	48.8%
	Freight trips (million)	0.11	0.03	0.01	0.01	0.06
	% in freight trips	100%	27.3%	8.8%	9.3%	54.5%
PM peak	Passengers trips (million)	2.84	0.93	0.25	0.26	1.40
	% in passenger trips	100%	32.7%	8.8%	9.2%	49.3%
	Freight trips (million)	0.44	0.15	0.05	0.04	0.20
	% in freight trips	100%	34.1%	11.2%	9.3%	45.5%

Table 4
Toll rates for distance- and cordon-based schemes.

Entrance time	Distance-based toll (USD/km)				Cordon-based toll (USD/entry)			
	Car	LGV	HGV	VHGV	Car	LGV	HGV	VHGV
07:30–07:55	0.16	0.24	0.32	0.4	1.65	2.50	3.25	4.05
07:55–08:00	0.26	0.38	0.51	0.64	2.60	3.90	5.20	6.50
08:00–10:00	0.32	0.48	0.64	0.8	3.25	4.90	6.50	8.10
10:00–10:05	0.26	0.38	0.51	0.64	2.60	3.90	5.20	6.50
10:05–10:30	0.16	0.24	0.32	0.4	1.65	2.50	3.25	4.05
15:30–15:55	0.14	0.2	0.27	0.34	1.50	2.25	3.00	3.25
15:55–16:00	0.22	0.32	0.43	0.54	2.50	3.60	4.80	6.00
16:00–19:00	0.27	0.41	0.54	0.68	3.00	4.50	6.00	7.50
19:00–10:05	0.22	0.32	0.43	0.54	2.50	3.60	4.80	6.00
19:05–19:30	0.14	0.2	0.27	0.34	1.50	2.25	3.00	3.25

and the second term represents the average queuing delay of a vehicle during the five-minute interval. Link-level MCTs can be computed by summing up the associated segment-level MCTs.

From Eq. (11), we can compute the total MCT for a given trip within the tolled area, by summing up the link-level MCTs (computed at the time-interval corresponding to entry on the link) for all component links on the path within the tolled region. In the case of the distance-based tolling policy, we can compute the toll tariff per unit distance as the total MCT for all tolled trips in the specific time period (for example, AM peak) divided by the total trip distance in this period. Similarly, in case of the cordon-based policy the toll rate is computed as the total MCT of tolled trips divided by the number of tolled trips. Finally, for the area-based scheme, the toll rate is the total MCT divided by the total number of vehicles traveling in the specific time-period within the region.

The design toll rates based on the computed MCTs from the baseline simulation are summarized in Table 4 for the distance- and cordon-based schemes. We employ a step-toll profile similar to that implemented in Stockholm and Singapore. The two shoulders before and after the peak-period avoid an abrupt discontinuous increase in the toll from 0 to the peak-period value. For the area-based scheme, the tolls are computed to be $2.65, 4, 5.5$ and 6.6 USD for cars, LGVs, HGVs, VHGVs, respectively. The tolls are flat and apply to any vehicle traveling within the area between the period from 8 AM to 7 PM.

The design tolls rates for the cordon-based scheme appear reasonable in comparison with several examples from practice: the ERP scheme in Singapore (0.37–4.41 USD), the Milan Area C scheme (2.35–5.87 USD), Motorway Essingeleden from Solna to Stockholm in Sweden (2.27–3.40 USD), and SR520 serving downtown Seattle (3.40–4.30 USD). For distance-based pricing policies, the few examples from practice in an urban setting largely target long-haul heavy vehicles, for example, motorways in Germany (7.5–11.99 tons: 0.11–0.20 USD/km) and Belgium, city zone (3.5–12 tons: 0.12–0.22 USD/km). Finally, for the area-based scheme, as of June 2021, London's congestion charge zone covering 0.14 million residents and 20.7 sq km. charges 20.92 USD from 7 AM to 10 PM, 7 days a week. Given that our toll area is much larger and population density much smaller, the toll rates are considerably lower in comparison.

We caution that computational intractability prevented us from carrying out a comparison of welfare maximizing designs of the three schemes, i.e., a comparison of optimized second-best schemes (see for example, Anas and Hiramatsu (2013)). Our results should be interpreted keeping this in mind.

5.5. Performance measures

5.5.1. Social welfare

The total social welfare, denoted by SW is given by,

$$SW = PS + CS + GR - EC, \tag{12}$$

where PS denotes the producer surplus, CS, the consumer surplus, GR, the government revenue (from tolls, fuel taxes and transit fares), and EC, the emission costs.

Government Revenue: We assume that the government or regulator operates the toll system and public transit and collects fuel taxes. The agency's revenue consists of three components: toll earning, public transit fare collection, and fuel tax revenue collected from passenger and freight vehicles. The toll earning is the toll revenue minus depreciation and operation costs, for which, we use a lower bound from various estimates — 27% of the toll revenue (Kirk, 2017).

Consumer Surplus: In our context, passenger travelers are the consumers. For passengers, we use a disaggregate utility-based accessibility measure originating from random utility theory. The accessibility measure of individual n, denoted A_n equals the expected maximum utility $E(U_{an})$, which can be expressed as a logsum of the utilities over all alternative activity patterns and is given by,

$$A_n = E(U_{an}) = \frac{1}{\mu}\ln\left[\sum_{a\in C_n} exp(\mu V_{an})\right], \tag{13}$$

where, V_{an} is the systematic component of utility U_{an} of choosing an activity pattern a from a set of alternative patterns C_n. The Activity-Based Accessibility measure (ABA) is obtained from the top of the hierarchical model structure (day pattern level, see Fig. 10) and is scaled with respect to cost and normalized to yield the consumer surplus:

$$ABA_n = \alpha_{nx}(A_n - A_n^0), \tag{14}$$

where A_n is the accessibility for individual n under a specific policy, A_n^0 represents the accessibility under an alternative baseline scenario, and the scaling factor is given by Dong et al. (2006),

$$\alpha_{nx} = \left(\frac{A_n^{\Delta x} - A_n}{\Delta x \sum_{j\in C_n} p_{jn} t_j}\right)^{-1}, \tag{15}$$

where $A_n^{\Delta x}$ represents the accessibility under a scenario where the cost is increased by Δx in all trips and activity schedules, C_n represents the set of all possible activity schedules for individual n, p_{jn} is the probability of individual n choosing activity pattern j, and t_j is the number of trips in activity pattern j. Note that we use the average per capita trip rate as an approximation of $\sum_{j\in C_n} p_{jn} t_j$ for all individuals (given its complexity to calculate). The passenger consumer surplus, denoted CS_P is the sum of all travelers' ABA:

$$CS_P = \sum_n ABA_n \tag{16}$$

Producer Surplus: The producers in our context are the freight agents. On the freight side, our analysis is shipper-centric. In effect, we consider the freight shipper, carrier and receiver as one entity in the welfare analysis. The freight producer surplus equals gross revenue minus cost. We assume that in the short run, the total gross revenue is not affected by congestion pricing, and thus, the change in producer surplus is solely determined by the change in logistics costs. On the one hand, this assumption implies that the commodity purchase and sales prices are not affected, which is reasonable since long-term decisions are out of our scope. On the other hand, we assume that B2C e-commerce demand changes more flexibly. We assume that shippers increase delivery fees to the tolled area (see Section 3.3.2) and hence, the B2C commodity demand would decrease. The shipper's revenue from B2C commodities decrease but it is compensated by the delivery fees collected, so the gross effect is unknown. We defer the detailed study of this to future research.

The daily TLC (total logistics cost) of a contract i (s denotes a shipment) belonging to shipper n is given by (refer De Jong and Ben-Akiva (2007) for details):

$$TLC_i = \sum_{s\in i}(T_s + Y_s) + \frac{D_i + I_i + K_i + Z_i}{period_i} \tag{17}$$

$$Transportation\ cost: T_s = c_s \tag{18}$$

$$Capital\ cost\ during\ transportation: Y_s = d \cdot t_s \cdot v^{com_i} \cdot q_i \tag{19}$$

$$Deterioration\ and\ damage\ cost: D_i = d \cdot j \cdot g \cdot v^{com_i} \cdot Q_i \tag{20}$$

$$Inventory\ holding\ cost: I_i = w^{com_i} \cdot q_i/2 \tag{21}$$

$$Capital\ cost\ of\ inventory: K_i = d \cdot v^{com_i} \cdot q_i/2 \tag{22}$$

$$Stockout\ cost: Z_i = (w^{com_i} + d \cdot v^{com_i}) \cdot z\sqrt{LT_i \cdot \sigma_{Q_i}^2 + Q_i^2 \cdot \sigma_{LT_i}^2} \tag{23}$$

To obtain an average weekday TLC, we simply divide the cost components D_i, I_i, K_i, Z_i by the length of the planning period $period_i$. Table 15 summaries the definitions and sources of parameters. The simulation outputs the daily transportation cost and travel time, which can be directly used to calculate the relevant cost components.

Table 5
Number of trips and travelers tolled by entry time.

	Entry time	Distance	Cordon	Area
Passenger trips (million)	AM	1.11	0.255	
	PM	1.42	0.181	
	All	2.57	0.436	3.78
Passengers (million)	AM	1.01	0.247	
	PM	1.17	0.202	
	All	1.82	0.447	2.42
Freight trips (thousand)	AM	75.3	13.1	
	PM	312	48.9	
	All	387	62.0	655
Freight vehicles (thousand)	AM	30.1	8.73	
	PM	104	27.2	
	All	124	32.5	182

Emission Costs: The last component of the total social welfare is emission cost — the social cost of CO2 emissions. It comprises a key negative externality. The conversion of CO2 emissions to cost is based on U.S. Environmental Protection Agency's estimate for 2020, equivalent to 58 USD/ton of CO2 (U.S. EPA, 2016). For details on the emission model, we refer the reader to Oke et al. (2020).

5.5.2. Network performance

The measures of network performance we use are (1) Vehicle-Kilometers-Traveled (VKT) categorized by passenger mode and freight vehicle type, and (2) Travel Time Index (TTI), which is the ratio of congested to free-flow travel time, at the trip level. Congestion in a specific time period is quantified via a trip-length weighted TTI for all trips occurring in the time period.

5.5.3. Travel/activity patterns and logistics operations

The indicators used to describe travel/activity patterns include number of trips by mode, number of activities by type, mode shares, trips patterns by time-of-day and trip length distributions. Indicators for logistic operations include shipment size and freight vehicle load factors (maximum shipment load in a tour divided by vehicle capacity, both measured by weight).

5.5.4. Day-to-day learning and stochasticity

The performance measures for a given scenario are computed after five iterations of the day-to-day learning process, which ensures consistency between zone-to-zone travel private/public transit travel times and waiting times used in the pre-day and those obtained from the supply simulation (see Section 3.4). The initial zone-to-zone travel times are already values from prior simulations and hence, five iterations suffice to attain a reasonable measure of consistency.

It is also worth noting that the extent of stochasticity across multiple simulations of an average day at convergence is relatively low with regard to the key aggregate performance measures of interest: number of passenger trips ($0.07\% - 0.2\%$), number of freight trips ($0.1\% - 4\%$), passenger VKT ($0.09\% - 0.2\%$), freight VKT ($0.2\% - 0.5\%$). The magnitude of differences across scenarios should be interpreted in the context of the above numbers.

6. Results and discussion

Table 5 summaries the number of trips and the number of travelers tolled by trip's entrance time, grouped into the AM peak (AM), PM peak (PM), and the entire day (ALL). A passenger tour refers to a home-based tour, which involves a journey to and from a primary activity. Trips refer to segments of the tour between successive activities. A freight tour on the other hand represents a sojourn of a vehicle from the depot to a sequence of stops and back to the depot. A freight trip is the individual segment between two successive stops.

Recall that the toll period under Area is from 8 AM to 7 PM, which is longer than the other schemes (7:30 AM to 10:30 AM and 3:30 PM to 7:30 PM). For passengers, 52.6% of the population are tolled under Area, 39.6% of the population are tolled under Distance, whereas only 9.7% of the population are tolled under Cordon. Similarly, among all carriers who have at least one shipment, a greater percentage is tolled under Area (81.4%) than Distance (57.8%), and significantly more than Cordon (15.9%). We thus expect that the Cordon scheme would have a significantly smaller overall impact. Recall that we set upper bounds for the maximum daily toll for Distance policy — 10 USD for passenger car, 15 USD for LGV, 20 USD for HGV, and 25 USD for VHGV. It shows that 10.1% of tolled passenger cars, 4.5% of tolled LGVs, 13.4% of tolled HGV, and 16.7% of tolled VHGV reached this upper bound.

Among the travelers who pay tolls, the average tolls paid are summarized in Table 6. The average toll per passenger, per freight vehicle, as well as per freight carrier are highest for the Distance-based scheme followed by the Cordon-based and Area schemes, respectively. The total toll revenue on an average weekday is 7.53 million USD under Distance, 1.56 million USD under Cordon, and 7.22 million USD under Area. To put these numbers in context, the realized toll revenues on an average day observed under

Table 6
Average tolls paid (USD).

	Distance	Cordon	Area
Per passenger	3.31	2.79	2.65
Per LGV	8.56	5.42	4.00
Per HGV	11.52	6.15	6.00
Per VHGV	15.30	7.83	7.50
Per freight carrier	19.54	11.84	9.35

Table 7
Welfare gains under different scenarios relative to baseline (USD).

Category	Component (M USD/weekday)	Scenario		
		Distance	Cordon	Area
Change in producer surplus	Toll earning	+5.50	+1.14	+5.27
	Public transport revenue	+0.0545	+0.0124	+0.0586
	Fuel tax revenue	−0.0864	−0.0152	−0.0872
Change in consumer surplus	Passengers	−3.44	−1.01	−3.73
	Freight shippers/carriers	−0.167	−0.0529	−0.228
Change in emission costs	CO2 emissions	−0.412	−0.0932	−0.445
Change in total social welfare		+2.27	+0.167	+1.72

the Stockholm congestion charging scheme in 2006 was around 0.68 million USD[5] (Eliasson et al., 2009) (this increased two-fold in 2016, see Börjesson and Kristoffersson (2018)). The corresponding figures for Singapore in 2015 were approximately 0.59 million USD[6] (2022 USD) and annual revenues from the London congestion charging scheme in 2018 were around 300 million USD.[7]

6.1. Welfare

Table 7 summarizes the change in total social welfare compared against the base scenario for an average weekday, expressed in million USD. Clearly, the congestion pricing policies reduce the use of private vehicles and encourage public transit ridership, thus improving public transport revenue and reducing fuel tax revenue. We can also observe that in fact the toll revenues are significantly higher than the changes in consumer surplus or net user benefits (for both passenger and freight agents), for all the three pricing schemes. This finding is consistent with the literature, for example, Eliasson and Mattsson (2006) quantified the net total benefits to revenue ratio (assuming toll revenues are refunded uniformly through a lump sum allocation) from the Stockholm congestion charging scheme to be 0.32, while De Palma et al. (2005) reported a net benefit to total revenue ratio of 0.28 for a cordon scheme. The ratio of change in social welfare to toll revenues are 0.30 (2.27/7.53), 0.11 (0.167/1.56) and 0.238 (1.72/7.22) for the distance, cordon and area schemes, respectively. Overall, all three pricing policies improve overall welfare.

In terms of the relative performance of the three pricing schemes, the distance-based scheme outperforms the other two (gross social welfare of 2.27 million USD versus 1.72 and 0.167 for the area and cordon schemes). The distance-based scheme clearly internalizes congestion externalities more effectively by charging higher for longer trips that contribute more to congestion. This finding of the superiority of distance-based scheme relative to access- and area-based schemes has been reported for stylized networks and bottleneck models in the literature (Lehe, 2017; Liu et al., 2022). Lentzakis et al. (2020) also arrive at similar conclusions, estimating significantly higher welfare gains for a distance-based scheme relative to a cordon scheme. Comparing the distance-based and area-based schemes, we find that although the gross welfare improvements are relatively close, the reduction in consumer surplus is smaller under Distance (passengers: −3.44 million USD, freight: −0.167 million USD) compared with Area (passengers: −3.73 million USD, freight: −0.228 million USD). Finally, we note that part of the reason for the poor performance of the cordon scheme may be its design; it is plausible that higher benefits may be attained if there is a second cordon is closer to downtown Boston.

A third observation that we make is that the overall net benefits (prior to any refunding or use of the toll revenues) are negative for both passenger and freight agents, implying that the overall value of gains in travel time are smaller than the total tolls paid. This finding is also consistent with the literature, see for example, Eliasson and Mattsson (2006) and De Palma et al. (2005). Nevertheless, it should be pointed out that in the case of passenger travel, the extent and type of heterogeneity can determine whether net user benefits (prior to the use of toll revenues) are positive or negative. For instance, Van Den Berg and Verhoef (2011b) show that congestion pricing can leave a majority of travelers better off even without redistribution of toll revenues. Chen et al. (2023) find that when the coefficient of variation in the value of time is large (exceeds around 0.5 in their experiments), the net user benefits start to become positive (even before accounting for the use of toll revenues). Similarly, He et al. (2021) and Lentzakis et al. (2023) find positive net benefits even prior to any toll revenue redistribution using large-scale simulation models.

[5] adjusted to 2022 USD amounts; https://www.bls.gov/cpi/.
[6] https://ops.fhwa.dot.gov/publications/fhwahop08047/02summ.htm; https://mothership.sg/2018/04/erp-history-20-years/, Accessed 23 August, 2022.
[7] https://content.tfl.gov.uk/tfl-annual-report-and-statement-of-accounts-2018-19.pdf; Retrieved 23 August, 2022.

Table 8
Distributional impacts — Passenger.

Profiles	All	Group 1	Group 2	Group 3	Group 4
Distance					
Range of daily surplus (USD/weekday)	[−13.1, 9.2]	[−13.1, −1.3)	[−1.3, 0)	[0, 1.3)	[1.3, 9.2]
Percentage in population	100%	22.8%	37.1%	33.3%	6.8%
Avg daily surplus (USD/weekday)	−0.84	−4.73	−0.33	0.28	4.1
Avg number of car trips with either OD in toll area during toll periods	0.554	0.725	0.561	0.454	0.431
Avg distance traveled by car within toll area during toll periods (km)	5.19	7.27	5.24	4.00	3.82
Proportion of households with work/education location in toll area	0.683	0.933	0.623	0.524	0.953
Proportion of work activities among all daily activities	0.272	0.238	0.257	0.282	0.420
Avg household income (thousand $/year)	86.31	79.24	86.51	87.15	105
Cordon					
Range of daily surplus (USD/weekday)	[−14.7, 3.75]	[−14.7, −1.3)	[−1.3, 0)	[0, 1.3)	[1.3, 3.75]
Percentage in population	100%	8.1%	34.2%	51.3%	6.3%
Avg daily surplus (USD/weekday)	−0.25	−6.0	−0.28	0.41	2.0
Avg number of car trips with either OD in toll area during toll periods	0.561	1.16	0.425	0.397	1.87
Avg number of car trips entering toll area during toll periods	0.0953	1.13	0.0108	0.000100	0.000179
Avg distance traveled by car within toll area during toll periods (km)	5.50	11.1	3.38	4.37	19.1
Proportion of households with work/education location in toll area	0.683	1.000	0.613	0.648	0.950
Proportion of work activities among all daily activities	0.272	0.181	0.262	0.276	0.416
Avg household income (thousand $/year)	86.3	78.0	84.5	86.7	105
Area					
Range of daily surplus (USD/weekday)	[−6.9, 10.1]	[−6.9, −1.3)	[−1.3, 0)	[0, 1.3)	[1.3, 10.1]
Percentage in population	100%	31.5%	27.9%	28.9%	11.7%
Avg daily surplus change (USD/weekday)	−0.93	−4.34	−0.33	0.34	3.63
Avg number of car trips with either OD in toll area during toll periods	0.820	1.16	0.304	0.348	2.30
Avg distance traveled by car within toll area during toll periods (km)	6.76	10.7	1.69	1.74	20.6
Proportion of households with work/education location in toll area	0.683	0.853	0.551	0.551	0.865
Proportion of work activities among all daily activities	0.272	0.254	0.270	0.268	0.334
Avg household income (thousand $/year)	86.3	82.5	86.3	88.4	91.5

Finally, in terms of emission costs, the area and distance-based schemes again yield significantly larger benefits (reduction of 0.445 and 0.412 million USD per weekday) compared to the cordon scheme.

6.2. Distributional impacts — passenger

Distributional impacts have long been a focal point of political opposition to congestion pricing. Pricing may viewed as being 'unfair' if it is seen as disproportionately benefiting high income groups and burdening low income groups (Eliasson, 2016). Our analysis of distributional outcomes implicitly assumes that value of time is correlated with income and that there is a one-to-one relationship between VOT and income. Verhoef and Small (2004) have cautioned against viewing the VOT distribution as simply representing the income distribution since empirical studies have identified other correlates of income (see also (Lehe, 2020) on this). Nevertheless, due to the lack of sufficient data on this, as is standard practice, we assume that VOT is correlated with income.

With microsimulation, we can compute each individual's change in daily surplus and thus, identify "winners" and "losers" under congestion pricing by describing profiles of passengers belonging to groups with different ranges of daily surplus change. The definition of these groups is based on the assumption that a daily change in user benefits (surplus) of ±0.50 USD per trip can be considered small (with an average trip rate of 2.6, this implies a daily surplus change within ±1.30 USD per day). Under the distance-based scheme (Table 8), group 1 loses between 13.1 to 1.3 USD/person/weekday and group 4 gains from 1.3 to 9.2 USD/person/weekday while group 2 and group 3 are relatively less affected with changes of no more than 1.30 USD/person/weekday. Group 1 consists of 22.8% of the population, group 2 consists of 37.1%, group 3 consists of 33.3%, and group 4 is the minority, comprising 6.8%. Prior to the use of toll revenues, overall, 40.0% of the population benefit from the distance-based scheme while 60.0% are worse off.

Compared to the entire population, both group 1 (largest losses) and 4 (largest gains) have a high proportion of individuals with a fixed household work or education location within the toll area (93% and 95%, respectively). Interestingly, Group 4 have higher household income but make fewer and shorter trips on average (resulting in relatively lower tolls paid) and gain the most from the pricing scheme. As can be seen from Fig. 8, they also tend to reside close to the financial district in downtown Boston (lower panel in Fig. 8). In contrast, group 1 are more likely to stay outside the toll area or at the periphery, make more trips on average within the tolled area and have lower household incomes. In this regard, despite yielding the largest welfare gains, the current design of the distance-based scheme does appear to be regressive, as can be seen from the trend of increasing average incomes from group 1 to group 4. A lump-sum redistribution of toll revenues, while improving equity, will not guarantee Pareto improvement, nor will it make the scheme progressive. On the other hand, other avenues for use of the toll revenues, such as increasing public spending (to improve public transport or reduce car costs) or decreasing taxes will alter the distribution of benefits and have the potential to make the scheme progressive (see for example, Eliasson and Mattsson (2006)). Alternatively, other designs of the tariff scheme such as a two-part tariff may redress some of the inequities in the distribution of benefits given the large gains observed

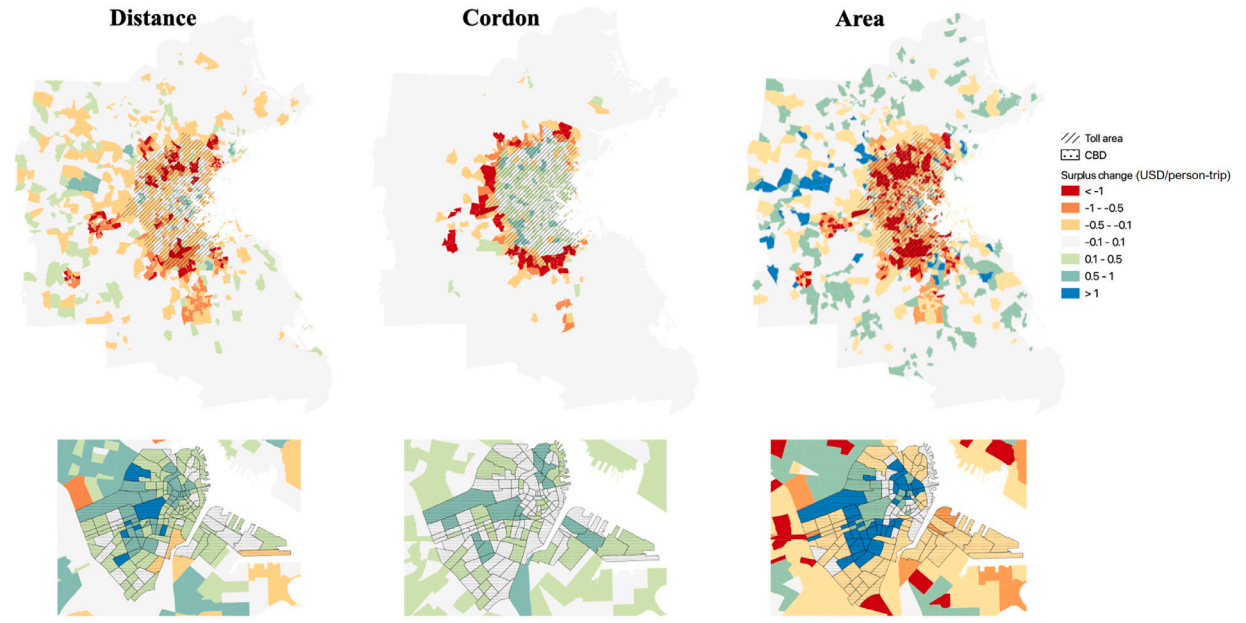

Fig. 8. Spatial distribution of passenger surplus (by household location).

for individuals with short trips and high incomes. Note that although the increasing trend in consumer surplus is associated with an increasing average income across the four groups, when considering individual travelers, the consumer surplus is not monotonic with the value of time. The non-monotonicity of consumer surplus (losses or gains) with respect to value of time has been reported for the bottleneck model (Van Den Berg and Verhoef, 2011b) and a static model with a mixed-bus alternative (Lehe, 2020).

Under the Cordon scheme, 57.7% of the population gain and 42.3% lose. Compared to the distance-based scheme, the proportion of big 'losers' (group 1) is much smaller due to the significantly smaller proportion of trips tolled. Concurrently, the proportion the large 'gainers' is also much smaller due to the significantly smaller travel time gains. Once again, as expected, both group 1 and group 4 are more likely to have a fixed household/work/education location in the toll area. Unlike the distance-based scheme, group 4 has a significantly large number of trips within the tolled area and these are almost exclusively internal trips that are not tolled but benefit from the travel time savings. In contrast, group 1 makes a higher number of entering trips (as expected) than the population average, thus incurring the toll cost. The cordon scheme also appears to be regressive, with an increase in average household income observed from group 1 to group 4. The large 'gainers' are high income households with an average annual income of around $105,000.

Under the area-based scheme, the proportions of large 'losers' and 'winners' are much higher than the other two scenarios. In the area-based scheme users pay a flat daily fee to travel within the tolled area, and thus, the individuals who gain the most tend to have a significantly higher number of trips in the tolled area than average. These are not necessarily those with the highest incomes living in the vicinity of downtown Boston, and thus the average incomes of the four groups are closer to each other than the other schemes. This can also be seen in Fig. 8, which shows that while the individuals who lose the most under the distance-based scheme tend to reside in the outer parts of the tolled region or outside the periphery, in the area-based scheme they tend to be distributed throughout the tolled region. Thus, the area-based scheme appears to be the least regressive amongst the three schemes.

6.3. Distributional impacts — freight

We perform a similar analysis for freight by describing profiles of shippers belonging to groups with different ranges of daily surplus change. As in the analysis of passengers, we divide shippers into four groups depending on their change in daily surplus under the different tolling schemes (see Table 9).

Under the distance-based scheme, the overall percentage of 'winners' and 'losers' is remarkably similar to the passenger case, with 40.9% of shippers gaining and 59.1% of shippers losing due to the pricing scheme. Although both group 1 and group 4 have a higher average number of shipments with an origin or destination in the tolled area (15.8 and 21.4, respectively, compared to the population average of 8.05), the average shipment value by weight of group 4 (16.8 $ per kg) is significantly higher than that of group 1 (8.76 $ per kg). Since the total logistics cost is positively correlated with shipment value by weight, given the same travel time savings, shippers with higher shipment values benefit more. Further, we also observe that group 1 has a smaller average employment size whereas group 4 has a significantly larger size, indicating that smaller business establishments tend to lose benefits. Thus, as in the case of passengers, the distance-based scheme also appears to be regressive with regard to distributional impacts on shippers.

Table 9
Distributional impacts — Freight.

Profiles	All	Group 1	Group 2	Group 3	Group 4
Distance					
Range of daily surplus change (USD/weekday)	[−322, 161]	[−322, −20.0)	[−20.0, 0)	[0, 20.0)	[20.0, 161]
Proportion in shipper establishments	100%	9.1%	50.0%	36.7%	4.2%
Avg daily surplus change (USD/weekday)	−3.85	−61.3	−4.59	3.28	66.3
Avg number of trips with either OD in toll area during toll periods	8.92	17.2	7.15	7.28	26.5
Avg distance traveled within toll area during toll periods (km)	64.2	154	48.3	51.3	174
Avg number of shipments with either OD in toll area	8.05	15.8	6.45	6.82	21.2
Avg shipment value by weight ($/kg)	11.4	8.76	10.3	12.8	16.8
Proportion of having establishment or pickup/delivery stops within toll area	0.664	0.992	0.615	0.613	0.993
Avg employment size	18.0	3.21	17.7	17.9	54.0
Cordon					
Range of daily surplus change (USD/weekday)	[−351, 87.2]	[−351, −20.0)	[−20.0, 0)	[0, 20.0)	[20.0, 87.2]
Proportion in shipper establishments	100%	4.4%	39.4%	53.0%	3.2%
Avg daily surplus change (USD/weekday)	−1.22	−86.2	−3.94	5.15	44.4
Avg number of trips with either OD in toll area during toll periods	9.10	24.9	7.32	7.72	32.1
Avg number of trips entering toll area during toll periods	1.43	17.3	0.730	0.441	4.58
Avg distance traveled within toll area during toll periods (km)	68.8	184	56.4	59.7	214
Avg number of shipments with either OD in toll area	8.05	18.9	6.54	6.72	33.7
Avg shipment value by weight ($/kg)	11.4	6.42	9.80	12.5	18.4
Proportion of having establishment or pickup/delivery stops within toll area	0.664	0.997	0.665	0.616	0.990
Avg employment size	18.0	1.71	16.5	17.8	61.5
Area					
Range of daily surplus change (USD/weekday)	[−223, 217]	[−223, −20.0]	[−20.0, 0)	[0, 20.0)	[20.0, 217]
Proportion in shipper establishments	100%	20.4%	29.7%	34.8%	15.2%
Avg daily surplus change (USD/weekday)	−5.26	−75.2	−3.68	4.23	63.8
Avg number of trips with either OD in toll area during toll periods	15.1	22.5	8.43	10.5	28.6
Avg distance traveled within toll area during toll periods (km)	116	133	69.1	78.4	268
Avg number of shipments with either OD in toll area	8.05	11.7	5.53	5.66	13.5
Avg shipment value by weight ($/kg)	11.3	10.1	9.43	12.7	13.5
Proportion of having establishment or pickup/delivery stops within toll area	0.664	0.990	0.482	0.484	0.990
Avg employment size	18.0	12.3	17.6	18.2	25.8

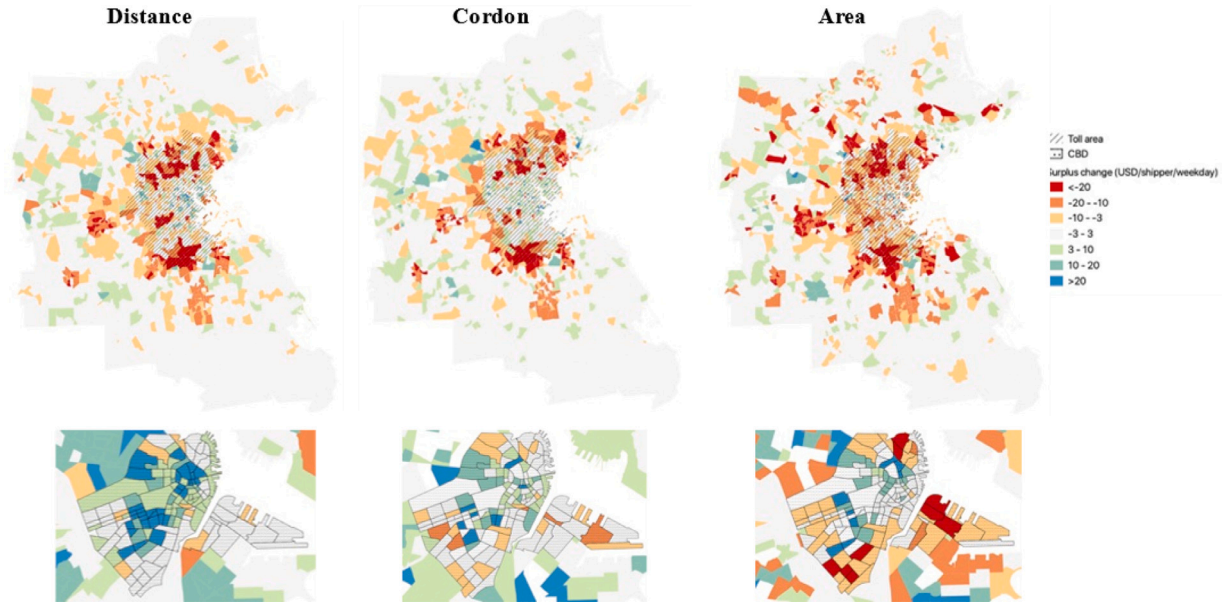

Fig. 9. Spatial distribution of freight surplus (by shipper location).

Under the Cordon scheme, 56.2% of shippers gain and 43.8% lose. As with the distance-based scheme, both group 1 and group 4 have a significantly higher number of trips with either the origin or destination in the tolled region. However, in case of group 4, a large percentage of these trips are internal trips that are not tolled whereas group 1 has a large percentage of trips that cross the

Table 10
VKT by vehicle type, OD pair, and departure time.

Time-of-day	Vehicle type	Internal trips				Connection trips			
		Base[a]	Distance	Cordon	Area	Base[a]	Distance	Cordon	Area
All day	Cars	27.03	−10.00%	1.50%	−5.00%	50.43	−5.20%	−0.70%	−2.60%
	LGV	1.46	−9.00%	−0.90%	−6.50%	2.49	−5.50%	−3.80%	−3.00%
	HGV	0.16	−11.20%	−0.40%	−7.90%	0.4	−6.00%	−3.90%	−3.00%
	VHGV	0.08	−10.60%	−2.10%	−5.50%	0.45	−6.90%	−2.60%	−2.90%
AM peak	Cars	4.68	−14.40%	2.40%	−3.80%	10.3	−8.30%	−3.10%	−1.70%
	LGV	0.16	−10.50%	−0.90%	−2.70%	0.34	−6.70%	−5.40%	−0.60%
	HGV	0.02	−13.40%	−1.70%	−5.00%	0.05	−6.60%	−4.70%	−0.50%
	VHGV	0.01	−11.20%	−1.00%	−4.20%	0.06	−8.20%	−5.00%	−1.80%
PM peak	Cars	6.22	−13.20%	1.90%	−4.10%	11.6	−8.00%	−1.40%	−1.90%
	LGV	0.64	−11.00%	−1.30%	−4.10%	1.14	−6.90%	−5.50%	−1.70%
	HGV	0.07	−12.60%	−0.70%	−5.60%	0.17	−8.10%	−6.40%	−1.90%
	VHGV	0.04	−14.60%	−0.70%	−7.20%	0.2	−7.70%	−7.40%	−3.40%

[a] Units: million kilometers.

cordon. Once again, the scheme appears to be regressive since shippers that benefit the most tend to be large establishments with a high shipment value.

Finally, under the area-based scheme, 50.0% of shippers gain and 50.0% lose. The profiles of the four groups suggest that the area-based scheme is less regressive than the distance and cordon schemes with the variation in average employment size and average shipment value being small across the four groups.

Part of the reason for the fact that smaller establishments lose and larger ones gain is that the capital cost during transportation (Eq. (19)) depends on the travel time savings and value of the commodity per unit weight. In general, the commodity values for larger establishments are relatively higher than that of the smaller establishments and thus, given the same travel time savings and tolls, the larger establishments gain more than the smaller ones. Thus, the commodity value has an analogous effect as the value of time does in the case of passengers.

Fig. 9 shows the average daily surplus change of shippers by shipper business establishment location. Observe that there are differences in the spatial patterns of daily surplus changes for freight agents and passengers. One explanation is that the shipper's establishment location is not necessarily a frequently visited stop, especially if the shipper does not use in-house fleets. This is also the reason why there can be establishments within the toll cordon under the cordon-based scheme that incur a negative surplus. A second explanation for the differences relative to the passenger case is the great variability in shippers' logistics operations, such as varying numbers of shipments, shipment values, fleet sizes, etc.

6.4. Network performance

The impacts of the tolling schemes on VKT are summarized in Table 10. The distance and area-based schemes both yield significant reductions in passenger car VKT overall (10% and 5%, respectively for internal trips and 5.2% and 2.6%, respectively for connection trips). As expected, the reductions in VKT in the distance-based scheme come solely from the peak periods (when the tolls are in effect) whereas for the area-based scheme they are distributed throughout the entire day. In both schemes, the reductions are larger for internal trips than connection trips, potentially due to a larger share of discretionary activities (which may be cancelled or performed at a location closer to home) in internal trips compared to connection trips. In contrast, the cordon-based scheme is far less effective, resulting in an overall VKT reduction of only 0.7% for connection trips, while in fact increasing the VKT of internal trips by 1.5%. This is the result of induced demand and destination changes of internal trips (which are not tolled) due to the reduced congestion within the cordon.

The impacts on freight VKT are more complex, being the combined result of changes in shipment size, ecommerce demand, vehicle operations planning and route choice. The relative reductions in freight VKT are once again the largest for the distance-based scheme for both internal and connection trips. Interestingly, internal the VKT of internal freight trips shows a reduction (although small) even under the cordon scheme despite the reduction of network congestion. The three schemes show differing impacts on VKT by vehicle type (LGV, HGV, VHGV).

In order to examine travel time improvements due to the pricing policies, we examine trips to, from and within the more congested central business district (CBD) within the toll area. The distance-weighted TTI for internal and connection trips to the CBD are summarized in Table 11. The distance-based scheme yields the highest reductions in TTI for internal trips (13.1% and 12.7% in the AM and PM peak, respectively) whereas the reductions in the area-based scheme are more modest (7.6% and 8.5%, respectively). The cordon-based schemes yields the smallest reductions in TTI (3.1% and 2.6% in the AM and PM peak, respectively). The trends for connection trips are similar.

6.5. Travel and activity patterns

In this section, we examine the impacts of the three pricing schemes on activity generation (passenger and freight), mode shares and departure time patterns.

Table 11
Travel Time Index (TTI) for CBD trips.

Period	Internal trips (CBD)				Connection trips (CBD)			
	Base	Distance	Cordon	Area	Base	Distance	Cordon	Area
AM peak	1.33	1.15 (−13.1%)	1.28 (−3.1%)	1.22 (−7.6%)	1.27	1.15 (−9.4%)	1.20 (−5.5%)	1.17 (−7.9%)
PM peak	1.28	1.12 (−12.7%)	1.25 (−2.6%)	1.18 (−8.5%)	1.21	1.11 (−8.1%)	1.16 (−4.0%)	1.11 (−8.7%)

Table 12
Impacts on departure time.

Mode	Internal trips				Connection trips			
	Base	Distance	Cordon	Area	Base	Distance	Cordon	Area
AM peak								
Car	16.4%	15.7% (−4.3%)	16.5% (+0.8%)	16.6% (+1.1%)	16.7%	16.2% (−3.1%)	16.2% (−3.1%)	16.8% (+0.9%)
PT	20.5%	21.2% (+3.1%)	20.3% (−1.1%)	20.3% (−1.2%)	18.8%	19.3% (+2.7%)	19.1% (+1.6%)	18.6% (−0.9%)
Freight	10.1%	10.0% (−1.2%)	10.1% (−0.0%)	10.5% (+3.9%)	11.1%	11.0% (−0.8%)	10.9% (−1.8%)	11.4% (+2.2%)
PM peak								
Car	22.9%	22.1% (−3.3%)	23.0% (+0.4%)	23.1% (+0.9%)	23.8%	23.1% (−2.8%)	23.5% (−1.1%)	24.0% (+0.7%)
PT	27.1%	27.6% (+1.8%)	26.8% (−0.9%)	26.9% (−0.6%)	24.3%	24.8% (+1.8%)	24.4% (+0.1%)	24.2% (−0.8%)
Freight	44.0%	43.3% (−1.6%)	43.9% (−0.4%)	45.1% (+2.4%)	46.4%	45.9% (−1.0%)	45.4% (−2.2%)	46.9% (+1.0%)

6.5.1. Activity generation

As expected, under both the distance and area-based schemes, a significant reduction in discretionary activities (6.5% and 5.2% reduction in shopping activities, respectively) is observed in the tolled area. Work and education activities, which are typically less elastic are affected to a smaller extent. The impacts on activities are likely to have welfare effects (for example, on economic productivity and the labor market) that are not quantified in our model. Observe also that the design of the pricing scheme can impact the destination choices of shopping activities; for instance, under the distance-based scheme, we see a small increase in shopping activities (+0.7%) outside the tolled area.

In terms of e-commerce, we find a decrease in total demand in the tolled area alongside with an even greater decrease of e-commerce home-delivery orders. The total number of e-commerce orders decrease by 8.1% under the distance-based scheme, 2.3% under the cordon scheme, and 6.8% under the area-based scheme. The main driver for this decrease is the increased delivery fees for home-delivery, which increases by 7.1% under Distance, 1.8% under Cordon, and 5.6% under Area. The increase in pickup trips in counter-intuitive, since although pickup fees remain unchanged, the pickup trip is tolled which incurs extra costs. Overall, our results suggest that home-delivery becomes less preferred under the congestion pricing schemes for residents within the tolled area.

6.5.2. Mode shares

The prototype city we study is highly auto-dependent (around 80% in the Base scenario) but has a relatively high transit share (around 12%) compared to most North American cities. The distance-based and area-based schemes lead to the largest decreases in single occupancy trips for both internal trips (reduction in Car share by 3.5 and 2.8 share points, respectively) and connection trips (1.9 and 1.6 share points, respectively). The decreases are the result of small shifts to public transit and relatively larger shifts to car-pooling. The cordon-based scheme is less effective in inducing mode shifts, once again underscoring the importance of cordon design. Moreover, the cordon scheme in fact results in a small increase in internal car trips due to the reduction in network congestion within the tolled region. The total number of car trips reduces by around 192,000 (6.6%) under the distance-based scheme and 190,000 under the area-based scheme.

6.5.3. Departure-time patterns

Table 12 summarizes the impacts of the three pricing schemes on departure time patterns for both passenger and freight traffic. The distance-based scheme yields the largest reductions in the share of peak period travel (4.3% and 3.1% for internal and connection trips, respectively). The cordon-based scheme is equally effective in reducing the share of peak-period connection trips (3.1% decrease) but in fact causes a small increase in the percentage of peak-period internal trips due to the reduction in travel times within the tolled region. Interestingly, the area-based scheme is ineffective in causing a reduction in the share of peak-period travel due to the flat toll rate throughout the day, and in fact, leads to an increase in the share of both connection and internal peak-period trips. Thus, although overall VKT does reduce under the area-based scheme, a large part of this reduction comes from the off-peak period.

The departure time pattern of freight traffic is different from that of passengers — the proportion of AM peak trips is quite low (~16%) and most trips take place during mid-day and the PM peak (~44%). Under congestion pricing, freight trips departing in AM and PM peaks decrease under Distance but the relative magnitudes are smaller than that of passenger trips, due to lower cost elasticities. The percentage decrease is larger in the PM peak where most of the traffic occurs. Under Cordon and Area, the impacts are similar to that of passenger trips but with smaller magnitudes of change.

Table 13
Shipment size.

Type	Internal shipments				Connection shipments			
	Base	Distance	Cordon	Area	Base	Distance	Cordon	Area
All	149.3	153.9 (+3.1%)	151.0 (+1.1%)	154.2 (+3.3%)	154.3	156.4 (+1.4%)	156.3 (+1.3%)	158.8 (+2.9%)
Non-ecommerce	287.2	293.3 (+2.1%)	290.8 (+1.2%)	295.5 (+2.9%)	312.5	318.3 (+1.9%)	317.8 (+1.7%)	320.4 (+2.5%)
E-commerce	14.1	14.7 (+4.3%)	14.5 (+2.9%)	14.8 (+4.7%)	15.6	15.9 (+1.9%)	15.9 (+1.9%)	16.1 (+3.2%)

Table 14
Average freight vehicle load factor.

	Internal tours				Connection tours			
	Base	Distance	Cordon	Area	Base	Distance	Cordon	Area
All carriers								
LGV	51.2%	52.7% (+2.8%)	51.0% (−0.4%)	51.1% (−0.2%)	53.0%	54.0% (+1.9%)	53.5% (+1.0%)	53.2% (+0.3%)
HGV	49.3%	51.7% (+4.9%)	49.0% (−0.6%)	49.0% (−0.6%)	48.7%	49.7% (+2.0%)	49.4% (+1.4%)	49.0% (+0.7%)
VHGV	31.6%	33.4%(+5.9%)	31.5% (−0.3%)	31.1% (−1.6%)	35.8%	36.7% (+2.5%)	36.6% (+2.1%)	36.1% (+0.9%)
Large carriers								
LGV	71.7%	75.9% (+5.8%)	70.9% (−1.2%)	71.3% (−0.6%)	75.3%	78.7% (+4.4%)	77.3% (+2.7%)	76.2% (+1.1%)
HGV	64.9%	69.4% (+6.8%)	63.9% (−1.6%)	64.4% (−0.9%)	65.1%	69.2% (+6.4%)	67.4% (+3.6%)	67.0% (+3.0%)
VHGV	46.3%	51.7% (+11.7%)	45.4% (−1.8%)	46.0% (−0.6%)	54.3%	58.2% (+7.2%)	57.0% (+5.1%)	56.0% (+3.3%)

6.6. Logistics operations

6.6.1. Shipment size

Table 13 shows the average shipment size by weight (kg) for different shipment types (B2B non-ecommerce or B2C e-commerce shipments) and shipment OD pairs. All the three pricing schemes result in an increase in shipment weight, although by differing magnitudes. Since the total commodity production and consumption is assumed to be fixed, a larger shipment size implies a lower shipment frequency and hence, a decrease in freight vehicle trips. For e-commerce shipments, which are significantly smaller than non-ecommerce shipments in size, this relative size increase is more significant. The increase is the most significant under the area-based and distance-based schemes whereas the changes are relatively small under the cordon-based scheme.

6.6.2. Freight vehicle load factor

The average freight vehicle load factors across all tours by vehicle type (LGV, HGV, and VHGV) are summarized in Table 14. The OD pairs are the ODs of the first trip of the vehicle's tour. Overall, the freight vehicle load factors are quite low for all vehicle types (~50% for LGV and HGV, 32%–36% for VHGV) in the base scenario, indicating low operational efficiency. The load factors increase significantly only under Distance, which results in an increase in load factors of internal and connection tours by 2%–6%.

In the VOP model, we consider 3 constraints in shipment-to-vehicle assignment and tour formation: shipment time window, vehicle capacity, and vehicle maximum working hours. In the case of tour termination, we find a majority are due to the shipment time window constraint (26.3%) and having no more shipments left (57.9%). This might partly explain why carriers do not further consolidate shipments to one vehicle. We then select a subset of "large carriers" who have sufficiently large fleets and large numbers of shipments to be carried (>100 shipments). For these carriers, the change in vehicle load factor is much more significant (Table 14) compared to the entire carrier population under congestion pricing. Among the three freight vehicle types, in most cases the percentage increase in load factor is $VHGV > HGV > LGV$, indicating that for the $VHGV$ vehicle type with the highest toll rate, the load needs to be sufficiently improved than the status quo for the carriers to opt to use it.

6.6.3. Freight tour time per shipment

Total freight tour time is mainly dependent on two factors. The first is the number of stops per tour. Carriers could increase the number of trips per tour yielding a shorter travel distance per shipment and hence, a reduced transportation cost under congestion pricing. However, due to the increase in shipment size, the shipment frequency and thus the total trip demand decreases. These two effects of pricing counteract with each other and make the implication on the number of trips per tour somewhat ambiguous. The second factor is the average travel time per trip, which under pricing should decrease on average. The average distance per trip is predominantly dependent on the pickup and delivery locations, most of which the carriers cannot determine, but with careful planning, they can reduce the average trip distance yielding cost savings. We examine the freight tour time per shipment, which quantifies to some extent the efficiency of the tour. The results show that the largest percentage decreases in tour time per shipment are for LGV vehicles, with a decrease of around 6% in the peak periods under the distance-based scheme and around 3.5% under the area-based scheme.

7. Conclusions

This paper examines the impacts of several congestion pricing schemes (distance-based, area-based and cordon) on both passenger transport and freight in an integrated manner. We employ the agent- and activity-based microsimulator SimMobility, which explicitly simulates the behavioral decisions of the entire population of individuals and business establishments, dynamic multimodal network performance, and their interactions.

Simulations of a prototypical North American city with 4.6 million individuals and 0.130 million business establishments indicate that the distance-based scheme yields higher welfare gains (around 2.27 million USD per weekday) compared to the area-based (1.72 million USD per weekday). In line with several prior studies we find that the overall welfare gains are a modest fraction of toll revenues (30%, 24% and 11% for the distance-based, area-based and cordon schemes, respectively). All three schemes are regressive with regard to both individuals and shippers, although the area-based scheme fares relatively better than the distance-based and cordon-schemes in terms of distributional impacts. The distance- and area-based schemes yield significant reductions in both VKT (10% and 5%, respectively for internal trips and 5.2% and 2.6%, respectively for connection trips) and peak-period travel time indices (by up to 13.1% and 8.5%, respectively).

Overall, given that the overall welfare gains are dwarfed by the toll revenues, we concur with Anas (2020), Eliasson and Mattsson (2006) and Santos and Rojey (2004) who point out that ultimately, the outcomes from pricing depend in large part on how the toll revenues are used. In this regard and given our findings on the regressivity of all three schemes, a critical area for future research is in the design of suitable revenue recycling schemes that guarantee Pareto improvement. This would to a large degree placate public and political opposition. Tradable credit schemes also hold promise in this context since in principle, distributional outcomes and equity impacts can be appropriately influenced by the initial allocation of credits (de Palma et al., 2018; Seshadri et al., 2022; Chen et al., 2023).

There are several limitations of our analysis. First, it has focused solely on the transportation system as opposed to more complete general equilibrium approaches (for example Anas (2020)). De Palma and Lindsey (2011) note that labor markets are distorted by income taxes, which have implications for pricing of commuting trips, and these effects (among others) may have first-order importance. Second, we assume operating costs are a fixed percentage of toll revenues under the different schemes. Differing operating and transaction costs may significantly affect the overall welfare of the different schemes and their comparative performance. Third, our modeling of the interplay between passenger and freight is limited to interactions and congestion effects on the network. Substitution and/or complementarity effects between in-person shopping and online-shopping should be considered when determining the overall impacts of e-commerce. Finally, our calculations of producer surplus are shipper-centric and do not consider the complex relationships between shippers, receivers and carriers.

CRediT authorship contribution statement

Peiyu Jing: Conceptualization, Data curation, Formal analysis, Investigation, Methodology, Software, Writing – original draft. **Ravi Seshadri:** Conceptualization, Formal analysis, Investigation, Methodology, Project administration, Supervision, Writing – original draft, Writing – review & editing. **Takanori Sakai:** Conceptualization, Data curation, Formal analysis, Investigation, Methodology, Software, Writing – original draft, Writing – review & editing. **Ali Shamshiripour:** Investigation, Methodology, Project administration, Supervision, Writing – review & editing. **Andre Romano Alho:** Investigation, Methodology, Project administration, Supervision. **Antonios Lentzakis:** Formal analysis, Investigation, Methodology. **Moshe E. Ben-Akiva:** Conceptualization, Funding acquisition, Methodology, Project administration, Supervision.

Acknowledgments

This research was funded by Cintra S. A.

Appendix A. Pre-day activity-based model system

The structure of the pre-day model system is shown is Fig. 10.

Appendix B. Parameters in logistics cost function

The definitions and sources of parameters used in the computation of the logistics cost are summarized in Table 15.

Appendix C. Path size factor

To define the path size factor, we use an assignment matrix A_i to represent each VOP alternative i (omitting carrier subscript n for simplicity):

$$A_i = \begin{pmatrix} a_{1,1,i} & \cdots & a_{1,V,i} \\ \vdots & \ddots & \vdots \\ a_{S,1,i} & \cdots & a_{S,V,i} \end{pmatrix} \tag{24}$$

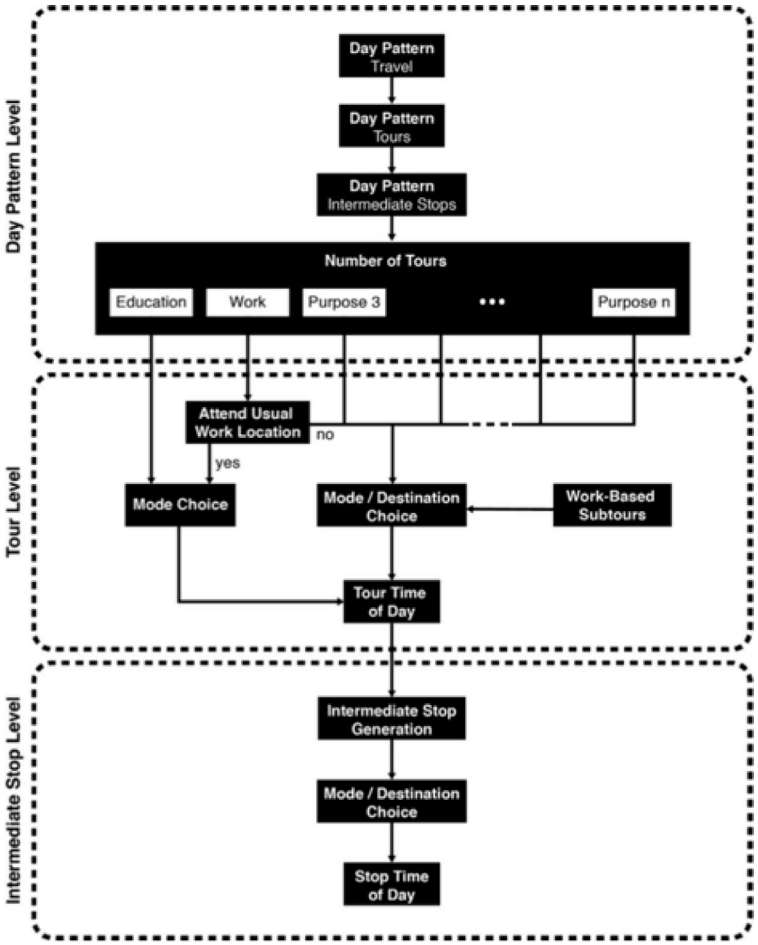

Fig. 10. Pre-day activity-based model system.

Table 15
Parameters in the logistics cost function.

Notation	Description	Value
c_s	Transportation cost	The systematic component of the VOP model is used as the cost function. Distance, time, and toll values are obtained from the within-day simulation.
d	Discount rate of cash	0.75% per year based on the 2021 secondary credit rate in Boston, Massachusetts.
t_s	Transportation time	Obtained from the within-day simulation (specified in units of years).
v^{com_i}	Commodity-type-specific value per unit of weight	Estimated using the 2012 micro-sample of the U.S. Commodity Flow Survey.
Q_i	Total demand by weight	Simulated from commodity contract or e-commerce model; unit is kg per contract period.
j	Shrinkage rate	Assumed as 1%.
g	Average period to receive an insurance claim	Assumed as 26.7 days (specified in units of years).
w^{com_i}	Storage cost per unit of weight	Refer to Eq. (3).
q_i	Shipment size of by weight	Simulated from shipment frequency & size model or e-commerce model.
z	z-score	Assumed as 1.03 (85% of cycles without shortage).
LT_i	Lead time	$LT_i = t_{s_i} + otherLT_i$. $otherLT_i$ are assumed as follows: 2 weekdays for B2C and 6 weekdays for B2B.
$\sigma^2_{Q_i}$	Variance of demand	Assumed 0 for B2B and obtained from the e-commerce simulation for B2C.
$\sigma^2_{LT_i}$	Variance of lead-time	Assume two components are uncorrelated, then $\sigma^2_{LT_i} = \sigma^2_{t_{s_i}} + \sigma^2_{otherLT_i}$. $\sigma^2_{t_{s_i}}$ is obtained from the within-day simulation. $\sigma^2_{otherLT_i}$ is assumed as 0.5 (translated into units of years when calculating stockout costs).

where $a_{s,v,i}$ is an element in assignment matrix A_i, which takes a value 1 if shipment s is assigned to vehicle v and 0 otherwise, S is total number of shipments to be assigned by the carrier, and V is the total number of vehicles in the carrier's fleet.

Each shipment is assigned to one vehicle, so we have,

$$\sum_{v=1,\ldots,V} a_{s,v,i} = 1, \forall s = 1, 2, \ldots, S, \forall i = 1, 2, \ldots |C_n|, \tag{25}$$

where C_n is the choice set of carrier n.

The overlap factor (denoted OF) for a VOP alternative i is defined as:

$$OF_i = 1/S \times \sum_{\{s,v|a_{s,v,i}=1\}} \frac{1}{\sum_{k=1,2,\ldots|C_n|} a_{s,v,k}} \tag{26}$$

The less an alternative overlaps with others in the choice set, the bigger its overlap factor is, and the maximum value it can take is 1. Conversely, the more an alternative overlaps with the others, the smaller its overlap factor, and the minimum value it can take is $1/S$.

Appendix D. Supplementary data

Supplementary material related to this article can be found online at https://doi.org/10.1016/j.tra.2024.104118.

References

Adnan, M., Pereira, F.C., Azevedo, C.M.L., Basak, K., Lovric, M., Raveau, S., Zhu, Y., Ferreira, J., Zegras, C., Ben-Akiva, M., 2016. Simmobility: A multi-scale integrated agent-based simulation platform. In: 95th Annual Meeting of the Transportation Research Board Forthcoming in Transportation Research Record. Vol. 2, The National Academies of Sciences, Engineering, and Medicine Washington, DC.

Anas, A., 2020. The cost of congestion and the benefits of congestion pricing: A general equilibrium analysis. Transp. Res. B 136, 110–137.

Anas, A., Chang, H., 2023. Productivity benefits of urban transportation megaprojects: A general equilibrium analysis of grand Paris express. Transp. Res. B 174, 102746.

Anas, A., Hiramatsu, T., 2013. The economics of cordon tolling: General equilibrium and welfare analysis. Econ. Transp. 2 (1), 18–37.

Anas, A., Lindsey, R., 2011. Reducing urban road transportation externalities: Road pricing in theory and in practice. Rev. Environ. Econ. Policy.

Anas, A., Liu, Y., 2007. A regional economy, land use, and transportation model (relu-tran©): Formulation, algorithm design, and testing. J. Reg. Sci. 47 (3), 415–455.

Arnott, R., De Palma, A., Lindsey, R., 1990. Economics of a bottleneck. J. Urban Econ. 27 (1), 111–130.

Arnott, R., De Palma, A., Lindsey, R., 1994. The welfare effects of congestion tolls with heterogeneous commuters. J. Transp. Econ. Policy 139–161.

Auld, J., Hope, M., Ley, H., Sokolov, V., Xu, B., Zhang, K., 2016. POLARIS: Agent-based modeling framework development and implementation for integrated travel demand and network and operations simulations. Transp. Res. C 64, 101–116.

Ben-Akiva, M., Abou-Zeid, M., 2013. Methodological issues in modelling time-of-travel preferences. Transp. A: Transp. Sci. 9 (9), 846–859.

Ben-Akiva, M.E., Toledo, T., Santos, J., Cox, N., Zhao, F., Lee, Y.J., Marzano, V., 2016. Freight data collection using GPS and web-based surveys: Insights from US truck drivers' survey and perspectives for urban freight. Case Stud. Transp. Policy 4 (1), 38–44.

Ben-Akiva, M., Watanatada, T., 1981. Application of a continuous spatial choice logit model. Struct. Anal. Discrete Data Econ. Appl. 320–343.

Bhat, C.R., 1998. Analysis of travel mode and departure time choice for urban shopping trips. Transp. Res. B 32 (6), 361–371.

Bhat, C.R., 2000. Incorporating observed and unobserved heterogeneity in urban work travel mode choice modeling. Transp. Sci. 34 (2), 228–238.

Börjesson, M., Kristoffersson, I., 2018. The Swedish congestion charges: Ten years on. Transp. Res. A 107, 35–51.

Bowman, J.L., Ben-Akiva, M.E., 2001. Activity-based disaggregate travel demand model system with activity schedules. Transp. Res. A 35 (1), 1–28.

Chen, D., Ignatius, J., Sun, D., Goh, M., Zhan, S., 2018. Impact of congestion pricing schemes on emissions and temporal shift of freight transport. Transp. Res. E: Logist. Transp. Rev. 118, 77–105.

Chen, S., Seshadri, R., Azevedo, C.L., Akkinepally, A.P., Liu, R., Araldo, A., Jiang, Y., Ben-Akiva, M.E., 2023. Market design for tradable mobility credits. Transp. Res. C 151, 104121. http://dx.doi.org/10.1016/j.trc.2023.104121.

Circella, G., Alemi, F., 2018. Transport policy in the era of ridehailing and other disruptive transportation technologies. In: Advances in Transport Policy and Planning. Vol. 1, Elsevier, pp. 119–144.

Cookson, G., Pishue, B., 2017. Inrix global traffic scorecard. Inrix research.

De Jong, G., Ben-Akiva, M., 2007. A micro-simulation model of shipment size and transport chain choice. Transp. Res. B 41 (9), 950–965.

De Palma, A., Kilani, M., Lindsey, R., 2005. Congestion pricing on a road network: A study using the dynamic equilibrium simulator METROPOLIS. Transp. Res. A 39 (7–9), 588–611.

De Palma, A., Lindsey, R., 2011. Traffic congestion pricing methodologies and technologies. Transp. Res. C 19 (6), 1377–1399.

De Palma, A., Marchal, F., Nesterov, Y., 1997. METROPOLIS: Modular system for dynamic traffic simulation. Transp. Res. Rec. 1607 (1), 178–184.

de Palma, A., Proost, S., Seshadri, R., Ben-Akiva, M., 2018. Congestion tolling-dollars versus tokens: A comparative analysis. Transp. Res. B 108, 261–280.

Ding, C., Mishra, S., Lin, Y., Xie, B., 2015. Cross-nested joint model of travel mode and departure time choice for urban commuting trips: Case study in maryland–washington, DC region. J. Urban Plann. Dev. 141 (4), 04014036.

Dong, X., Ben-Akiva, M.E., Bowman, J.L., Walker, J.L., 2006. Moving from trip-based to activity-based measures of accessibility. Transp. Res. A 40 (2), 163–180.

Eliasson, J., 2016. Is congestion pricing fair? Consumer and citizen perspectives on equity effects. Transp. Policy 52, 1–15.

Eliasson, J., Hultkrantz, L., Nerhagen, L., Rosqvist, L.S., 2009. The stockholm congestion–charging trial 2006: Overview of effects. Transp. Res. A 43 (3), 240–250.

Eliasson, J., Mattsson, L.-G., 2006. Equity effects of congestion pricing: quantitative methodology and a case study for stockholm. Transp. Res. A 40 (7), 602–620.

Gu, Z., Liu, Z., Cheng, Q., Saberi, M., 2018. Congestion pricing practices and public acceptance: A review of evidence. Case Stud. Transp. Policy 6 (1), 94–101.

He, B.Y., Zhou, J., Ma, Z., Wang, D., Sha, D., Lee, M., Chow, J.Y., Ozbay, K., 2021. A validated multi-agent simulation test bed to evaluate congestion pricing policies on population segments by time-of-day in New York City. Transp. Policy 101, 145–161.

Hess, S., Bierlaire, M., Polak, J.W., 2005. Estimation of value of travel-time savings using mixed logit models. Transp. Res. A 39 (2–3), 221–236.

Holguín-Veras, J., 2010. The truth, the myths and the possible in freight road pricing in congested urban areas. Proc.-Soc. Behav. Sci. 2 (3), 6366–6377.

Holguín-Veras, J., 2011. Urban delivery industry response to cordon pricing, time–distance pricing, and carrier–receiver policies in competitive markets. Transp. Res. A 45 (8), 802–824.

Holguín-Veras, J., Wang, Q., Xu, N., Ozbay, K., Cetin, M., Polimeni, J., 2006. The impacts of time of day pricing on the behavior of freight carriers in a congested urban area: Implications to road pricing. Transp. Res. A 40 (9), 744–766.

Hummels, D.L., 1999. Toward a geography of trade costs. Available at SSRN 160533.
Jing, P., 2022. Design and evaluation of urban congestion pricing policies with microsimulation of passenger and freight (Ph.D. thesis). Massachusetts Institute of Technology.
Kaddoura, I., Nagel, K., 2019. Congestion pricing in a real-world oriented agent-based simulation context. Res. Transp. Econ. 74, 40–51.
King, D., Manville, M., Shoup, D., 2007. The political calculus of congestion pricing. Transp. Policy 14 (2), 111–123.
Kirk, R.S., 2017. Tolling US highways and bridges. In: Congressional Research Service Report.
Lehe, L.J., 2017. Downtown tolls and the distribution of trip lengths. Econ. Transp. 11, 23–32.
Lehe, L., 2019. Downtown congestion pricing in practice. Transp. Res. C 100, 200–223.
Lehe, L.J., 2020. Winners and losers from road pricing with heterogeneous travelers and a mixed-traffic bus alternative. Transp. Res. B 139, 432–446.
Lentzakis, A.F., Seshadri, R., Akkinepally, A., Vu, V.-A., Ben-Akiva, M., 2020. Hierarchical density-based clustering methods for tolling zone definition and their impact on distance-based toll optimization. Transp. Res. C 118, 102685.
Lentzakis, A.F., Seshadri, R., Ben-Akiva, M., 2023. Predictive distance-based road pricing—Designing tolling zones through unsupervised learning. Transp. Res. A 170, 103611.
Levinson, D., 2010. Equity effects of road pricing: A review. Transp. Rev. 30 (1), 33–57.
Liu, R., Chen, S., Jiang, Y., Seshadri, R., Ben-Akiva, M., Lima Azevedo, C., 2022. Managing network congestion with a trip-and area-based tradable credit scheme. Transp. B: Transp. Dyn. 1–29.
Lu, Y., Adnan, M., Basak, K., Pereira, F.C., Carrion, C., Saber, V.H., Loganathan, H., Ben-Akiva, M.E., 2015. Simmobility mid-term simulator: A state of the art integrated agent based demand and supply model. In: 94th Annual Meeting of the Transportation Research Board, Washington, DC.
Murray, D., Glidewell, S., 2020. An analysis of the operational costs of trucking: 2019 update.
National Institute for Land and Infrastructure Management, 2016. A Report on Vehicle Operations Efficiency. Technical Report, http://www.nilim.go.jp/lab/bcg/siryou/tnn/tnn0671pdf/ks067111.pdf.
Oh, S., Lentzakis, A.F., Seshadri, R., Ben-Akiva, M., 2021. Impacts of automated mobility-on-demand on traffic dynamics, energy and emissions: A case study of Singapore. Simul. Model. Pract. Theory 110, 102327.
Oh, S., Seshadri, R., Azevedo, C.L., Kumar, N., Basak, K., Ben-Akiva, M., 2020. Assessing the impacts of automated mobility-on-demand through agent-based simulation: A study of Singapore. Transp. Res. A 138, 367–388.
Oke, J.B., Aboutaleb, Y.M., Akkinepally, A., Azevedo, C.L., Han, Y., Zegras, P.C., Ferreira, J., Ben-Akiva, M.E., 2019. A novel global urban typology framework for sustainable mobility futures. Environ. Res. Lett. 14 (9), 095006.
Oke, J.B., Akkinepally, A.P., Chen, S., Xie, Y., Aboutaleb, Y.M., Azevedo, C.L., Zegras, P.C., Ferreira, J., Ben-Akiva, M., 2020. Evaluating the systemic effects of automated mobility-on-demand services via large-scale agent-based simulation of auto-dependent prototype cities. Transp. Res. A 140, 98–126.
Perera, H.L.K., 2019. Determining the Optimum Toll Level for Freight Vehicles in Urban Conditions (Ph.D. thesis). University of Melbourne.
Ramming, M.S., 2001. Network knowledge and route choice (Ph. D. Thesis). Massachusetts Institute of Technology, Unpublished.
Sakai, T., Alho, A.R., Bhavathrathan, B., Dalla Chiara, G., Gopalakrishnan, R., Jing, P., Hyodo, T., Cheah, L., Ben-Akiva, M., 2020b. SimMobility freight: An agent-based urban freight simulator for evaluating logistics solutions. Transp. Res. E: Logist. Transp. Rev. 141, 102017.
Sakai, T., Alho, A., Hyodo, T., Ben-Akiva, M., 2020a. Empirical shipment size model for urban freight and its implications. Transp. Res. Rec. 2674 (5), 12–21.
Sakai, T., Hara, Y., Seshadri, R., Alho, A.R., Hasnine, M.S., Jing, P., Chua, Z., Ben-Akiva, M., 2022. Household-based E-commerce demand modeling for an agent-based urban transportation simulation platform. Transp. Plann. Technol. 1–23.
Santos, G., Rojey, L., 2004. Distributional impacts of road pricing: The truth behind the myth. Transportation 31 (1), 21–42.
Santos, G., Verhoef, E., 2011. Road congestion pricing. In: A Handbook of Transport Economics. Edward Elgar Publishing.
Sasic, A., Habib, K.N., 2013. Modelling departure time choices by a heteroskedastic generalized logit (het-genl) model: An investigation on home-based commuting trips in the greater toronto and hamilton area (GTHA). Transp. Res. A 50, 15–32.
Schrank, D., Eisele, B., Lomax, T., Bak, J., et al., 2015. 2015 Urban mobility scorecard.
Seshadri, R., de Palma, A., Ben-Akiva, M., 2022. Congestion tolling—Dollars versus tokens: Within-day dynamics. Transp. Res. C 143, 103836.
Simoni, M.D., Kockelman, K.M., Gurumurthy, K.M., Bischoff, J., 2019. Congestion pricing in a world of self-driving vehicles: An analysis of different strategies in alternative future scenarios. Transp. Res. C 98, 167–185.
Tan, R., Adnan, M., Lee, D.-H., Ben-Akiva, M.E., 2015. New path size formulation in path size logit for route choice modeling in public transport networks. Transp. Res. Rec. 2538 (1), 11–18.
Toledo, T., Atasoy, B., Jing, P., Ding-Mastera, J., Santos, J.O., Ben-Akiva, M., 2020. Intercity truck route choices incorporating toll road alternatives using enhanced GPS data. Transp. A: Transp. Sci. 16 (3), 654–675.
Van Den Berg, V., Verhoef, E.T., 2011a. Congestion tolling in the bottleneck model with heterogeneous values of time. Transp. Res. B 45 (1), 60–78.
Van Den Berg, V., Verhoef, E.T., 2011b. Winning or losing from dynamic bottleneck congestion pricing?: The distributional effects of road pricing with heterogeneity in values of time and schedule delay. J. Public Econ. 95 (7–8), 983–992.
Vega, A., Reynolds-Feighan, A., 2008. Employment sub-centres and travel-to-work mode choice in the dublin region. Urban Stud. 45 (9), 1747–1768.
Verhoef, E.T., 2002. Second-best congestion pricing in general static transportation networks with elastic demands. Reg. Sci. Urban Econ. 32 (3), 281–310.
Verhoef, E., Nijkamp, P., Rietveld, P., 1996. Second-best congestion pricing: The case of an untolled alternative. J. Urban Econ. 40 (3), 279–302.
Verhoef, E.T., Small, K.A., 2004. Product differentiation on roads. J. Transp. Econ. Policy (JTEP) 38 (1), 127–156.
Viegas de Lima, I., Danaf, M., Akkinepally, A., De Azevedo, C.L., Ben-Akiva, M., 2018. Modeling framework and implementation of activity-and agent-based simulation: An application to the Greater Boston Area. Transp. Res. Rec. 2672 (49), 146–157.
W. Axhausen, K., Horni, A., Nagel, K., 2016. The Multi-Agent Transport Simulation MATSim. Ubiquity Press.
Waliszewski, J.M., 2005. Towards Understanding the Impacts of Congestion Pricing on Urban Trucking (Ph.D. thesis). Massachusetts Institute of Technology.
Yang, H., 1999. System optimum, stochastic user equilibrium, and optimal link tolls. Transp. Sci. 33 (4), 354–360.
Yang, H., Huang, H.-J., 1998. Principle of marginal-cost pricing: How does it work in a general road network? Transp. Res. A 32 (1), 45–54.
Yang, L., Zheng, G., Zhu, X., 2013. Cross-nested logit model for the joint choice of residential location, travel mode, and departure time. Habitat Int. 38, 157–166.
Zhang, H., Seshadri, R., Prakash, A.A., Antoniou, C., Pereira, F.C., Ben-Akiva, M., 2021. Improving the accuracy and efficiency of online calibration for simulation-based dynamic traffic assignment. Transp. Res. C 128, 103195.
Zhang, H., Seshadri, R., Prakash, A.A., Pereira, F.C., Antoniou, C., Ben-Akiva, M.E., 2017. Improved calibration method for dynamic traffic assignment models: Constrained extended Kalman filter. Transp. Res. Rec. 2667 (1), 142–153.
Zhang, X., Yang, H., 2004. The optimal cordon-based network congestion pricing problem. Transp. Res. B 38 (6), 517–537.